Check for updates

ADVANCED MATERIALS
www.advmat.de

Recent Advances in Functional Materials through Cellulose Nanofiber Templating

Meghan E. Lamm, Kai Li, Ji Qian, Lu Wang, Nathalie Lavoine, Reagan Newman, Douglas J. Gardner, Teng Li, Liangbing Hu, Arthur J. Ragauskas, Halil Tekinalp, Vlastimil Kunc, and Soydan Ozcan**

Advanced templating techniques have enabled delicate control of both nano- and microscale structures and have helped thrust functional materials into the forefront of society. Cellulose nanomaterials are derived from natural polymers and show promise as a templating source for advanced materials. Use of cellulose nanomaterials in templating combines nanoscale property control with sustainability, an attribute often lacking in other templating techniques. Use of cellulose nanofibers for templating has shown great promise in recent years, but previous reviews on cellulose nanomaterial templating techniques have not provided extensive analysis of cellulose nanofiber templating. Cellulose nanofibers display several unique properties, including mechanical strength, porosity, high water retention, high surface functionality, and an entangled fibrous network, all of which can dictate distinctive aspects in the final templated materials. Many applications exploit the unique aspects of templating with cellulose nanofibers that help control the final properties of the material, including, but not limited to, applications in catalysis, batteries, supercapacitors, electrodes, building materials, biomaterials, and membranes. A detailed analysis on the use of cellulose nanofibers templating is provided, addressing specifically how careful selection of templating mechanisms and methodologies, combined toward goal applications, can be used to directly benefit chosen applications in advanced functional materials.

1. Introduction

Advanced functional materials have allowed researchers to develop materials toward high-performance applications. These materials, inorganics and organic polymers, for example, can now be used to store chemical energy in batteries, produce scaffolds for tissue growth, and even fabricate membranes to trap greenhouse gases.[1] However, to produce many of these advanced materials, specific morphological structures, many of which imitate those found in nature, need to be obtained using synthetic materials. In the lab, templating is one of the preferred strategies to create specific morphologies and requires a delicate balance of thermodynamics and kinetics. Templating involves using one material, the template, to dictate a specific shape for another material with the desired morphology. The template assumes a specific shape and then a second material, the precursor, is introduced (**Figure 1**). The precursor

Dr. M. E. Lamm, Dr. H. Tekinalp, Dr. V. Kunc, Dr. S. Ozcan
Manufacturing Demonstration Facility
Energy and Transportation Science Division
Oak Ridge National Laboratory
2350 Cherahala Boulevard, Knoxville, TN 37932, USA
E-mail: lammme@ornl.gov; ozcans@ornl.gov

Dr. K. Li
Chemical Sciences Division
Oak Ridge National Laboratory
1 Bethel Valley Road, Oak Ridge, TN 37831, USA

Dr. J. Qian, Prof. T. Li
Department of Mechanical Engineering
University of Maryland
College Park, MD 20742, USA

Dr. L. Wang, Prof. D. J. Gardner
Advanced Structures and Composites Center
University of Maine
35 Flagstaff Road, Orono, ME 04469, USA

The ORCID identification number(s) for the author(s) of this article can be found under https://doi.org/10.1002/adma.202005538.

DOI: 10.1002/adma.202005538

Dr. L. Wang, Prof. D. J. Gardner
School of Forest Resources
University of Maine
5755 Nutting Hall, Orono, ME 04469, USA

Prof. N. Lavoine
Department of Forest Biomaterials
College of Natural Resources
North Carolina State University
Raleigh, NC 27695, USA

R. Newman
Department of Biomedical Engineering
Georgia Institute of Technology
Atlanta, GA 30332, USA

Prof. L. Hu
Department of Materials Science and Engineering
University of Maryland
College Park, MD 20742, USA

Dr. A. J. Ragauskas
Center for BioEnergy Innovation (CBI)
Oak Ridge National Laboratory
Oak Ridge, TN 37831, USA

 © 2021 Wiley-VCH GmbH

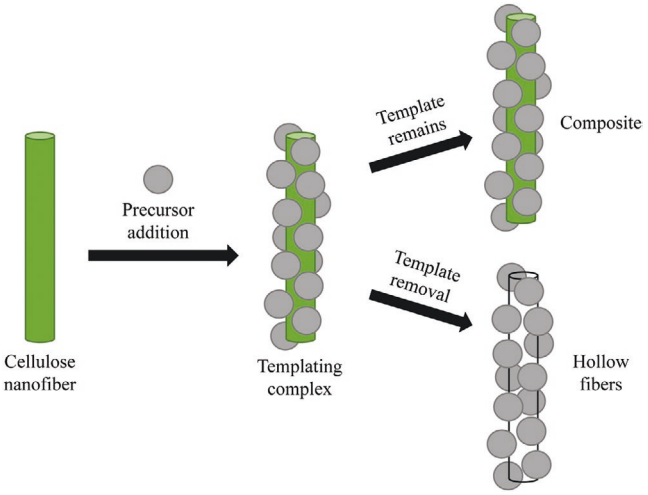

Figure 1. Graphical illustration depicting the process of templating.

is confined by the template and fills in the voids. In the final shape, these two materials can be kept, or the original template material can be removed.

A growing area in templating involves utilizing cellulose nanomaterials (CNs), including cellulose nanofibrils (CNFs), bacterial cellulose (BC), and cellulose nanocrystals (CNCs). Cellulose is a β-1,4-linkaged glucopyranoside polymer present in plant cell walls, which exists as a microfibril structure.[2,3] Cellulose nanofibers can be derived in two ways. The first involves mechanical fibrillation of cellulose fibers, typically from plant sources, into CNFs. The second involves synthesis of BC nanofibers through the bacterial fermentation of sugars. The cellulose nanofibers produced using these methods have similar aspect ratios, but differ in their specific dimensions, crystallinity, and chemical composition. CNFs typically have an aspect ratio >100 and a width of about 5–100 nm, whereas BC nanofibers have a similar width around 20–50 nm, but are slightly longer, averaging a few microns in length.[4] Alternatively, cellulose fibrils can undergo hydrolysis, typically with strong acids, to destroy the amorphous cellulose regions and produce highly crystalline CNCs. Comparatively, CNCs feature a rod-like shape with length around 150–200 nm and width of 5 nm. CNCs are another nanocellulose source used in templating, but other extensive reviews have already covered this method so it will therefore not be addressed in this review.[5,6,7,8–10]

CNs are a sustainable source for templating, can be easily removed through thermal treatment, display high specific surface area, and feature surface functional groups for ease of modification. Numerous works have focused on more traditional cellulosic materials as templates for constructing intricate structures, utilizing the inherent complexity that exists in those materials, including cellulose microfibrils (CMFs), regenerated cellulose, and cellulose derivatives.[11] In this review, the use of cellulose nanofibers (CNFs and BCs) as templating agents will be the focus.

Cellulose nanofibers feature a range of unique features that can be easily exploited during templating to produce beneficial properties in the resultant materials.[3] These features, such as high specific surface area, surface hydroxyl groups, ease of removal, and overall hydrophilicity of the materials, are shared among many of the CNs including CNCs. However, cellulose nanofibers also display some unique features. These nanofibers can undergo facile production of aerogels and foams due to its unique high water retention, which supports foaming. This property produces foams with not only high surface area, but a porous structure featuring pores on a variety of length scales. Additionally, cellulose nanofibers are mechanically robust and feature good flexibility, toughness, and strength. These combined mechanical properties are unique to cellulose nanofibers due to its long fibrillar morphology, which can create interconnect networks of fibers and allow for support of more complex morphologies during the templating process. It is a major goal of this review to connect these unique features inherent to cellulose nanofibers with promising properties in the resultant materials. Discussions will include introducing the mechanisms and methodologies useful in templating with cellulose nanofibers, as well as an in-depth analysis on the applications which utilize this templating strategy. These applications include batteries, catalysts, supercapacitors, biomaterials, building materials, and membranes, all of which exploit properties unique to cellulose nanofiber templating. This review will serve to present cellulose nanofibers as a promising templating material, which should help provide sustainable nanoscale control of advanced functional materials well into the future.

2. Templating Mechanisms and Methodologies toward Controlled Morphologies

The various forms of CNs provide a wide assortment of possible templating substrate architectures ranging from nanoscale to macroscale dimensions.[12] Examples of possible cellulose nanofiber template architectures include 1D particles or powders, 2D loosely arrayed fibrous mats or dense film structures, and last, 3D porous foams or hydrogel scaffolds. The variety of architectures allows for use as a

Dr. A. J. Ragauskas
Joint Institute for Biological Sciences
Biosciences Division
Oak Ridge National Laboratory
Oak Ridge, TN 37831, USA
Dr. A. J. Ragauskas
Department of Chemical and Biomolecular Engineering
University of Tennessee
Knoxville, TN 37996, USA
Dr. A. J. Ragauskas
Department of Forestry
Wildlife and Fisheries
Center for Renewable Carbon
The University of Tennessee Institute of Agriculture
Knoxville, TN 37996, USA
Dr. A. J. Ragauskas
Department of Mechanical
Aerospace, and Biomedical Engineering
University of Tennessee
Estabrook Road, Knoxville, TN 37916, USA

© 2021 Wiley-VCH GmbH

Table 1. Methodologies and mechanisms used in cellulose nanofiber templating, including advantages of each technique.

Methodology/mechanisms		Summary of technique	Common materials	Advantages of cellulose nanofibers	Refs.
Sacrificial templating		Template material is used to direct structure, removed by physical or chemical methods	Metal oxide, ceramics	Porous, high specific surface area, flexible, easily removed (physically or chemically)	[15–17]
Precursors	Generalized	Combine with template and undergo chemical reaction to form final desired material	Inorganics	Mechanically robust	[18,19]
	Electrospinning	Method to produce fibers using electric charge	Inorganics	Fibril morphology, hydroxyl groups, flexible, mechanically robust	[20,21]
	Atomic layer deposition (ALD)	A vacuum state method that deposits thin film sequentially using gas phase chemicals	Inorganics, ceramics	Mechanically robust, hydroxyl groups, porous, high surface area	[17,22]
	Layer-by-layer deposition (LBL)	Thin film deposition of alternating layers of opposite charged material	Inorganics, hybrid materials, polymers	Hydroxyl groups, high surface area, porous, mechanically robust	[23]
Liquid crystal templates		Use of inherent colloid formation to align template	Inorganics	Hydroxyl groups, aligned fibers, flexible	[24–27]
Co-templating		Template and active material undergo templating together to form final material	Hybrid materials	Hydrophilic, mechanically robust, stable	[28,29]
Sol–gel		Process that transforms precursors in liquid into a gel structure	Metal oxides	Hydroxyl groups, hydrophilic, high water retention	[15,26,30–34]
Foaming		Formation of stable porous structures that transform to aerogels after water removal	Inorganics	Porous, hydroxyl groups, high water retention, mechanical strength	[17,22,35–37]

templating agent with a multitude of materials for catalysis, drug release, batteries, magnets, filters, sensors, tissue scaffolds, and semiconductors.[3,6,13,14] The mechanisms and methodologies of templating are elaborated in the following sections and also summarized in **Table 1**. It is the authors' attempt to classify these templating mechanisms and methodologies found in literature and examine their usefulness in the templating with cellulose nanofibers. However, more than one mechanism or method may be applied at the same time in a single study. The introduction of these strategies will also include analysis of common materials used in these techniques, as well as the advantages of utilizing cellulose nanofiber materials.

2.1. Sacrificial Templating

In sacrificial templating, the substrate that is used to build the template or scaffold is removed by chemical or physical means, resulting in the particular material with desired structure.[38] Sacrificial templates are commonly used to impart porosity to gels. Since CNFs are inherently porous, materials can easily achieve high surface area with porosity over a range of scales. The chemical means of template removal is by use of a solvent that dissolves the template, which is usually done at near ambient conditions to retain delicate structures. For example, phenol-formaldehyde (PF) resin can be mixed with CNC suspension to yield an iridescent polymer composite film with tunable colors.[39] The CNC template was removed by alkaline treatment, creating a mesoporous PF film with high strength and flexibility, which common PF films do not possess. Similar facile chemical methods can easily be used to remove CNFs. Alternatively, with physical means, high temperatures are commonly used to thermally remove the template and leave the resulting structure, which is often used for metal oxides and ceramics.[15–17] For instance, a porous TiO_2/Fe_2O_3 nanocomposite was obtained by using the CNFs contained in filter paper as a template followed by calcinating the core CNFs.[16] The TiO_2/Fe_2O_3 nanocomposite tubes are potential new electrodes for lithium ion batteries. A similar approach was used for silica nanotubes with BC templating.[15] Since cellulose nanofibers can easily be removed with either method after templating is complete, their use in sacrificial templating is common practice.

2.2. Precursor

A precursor is a substance from which another is formed. With the various types of CNs available and the ability to form them into various structures reflecting different dimensionalities and size scales, there are numerous opportunities to create templates and scaffolds. One example is a carbon network derived from carbonized polyaniline (PANI) coated BC.[18] Incorporating MnO_2 nanoparticles on carbon nanofibers (CFs) can efficiently improve the electrochemical properties of the hybrid materials for supercapacitors. Compared to other carbon nanofibers, the carbonized BC-PANI carbon network is less expensive in cost, easy to fabricate, and has a lower environmental impact. Carbonized BC-PANI carbon networks provide conductive support for

© 2021 Wiley-VCH GmbH

integrated active electrode materials, which exhibit higher energy density than other common MnO_2-porous carbon supercapacitors. In another study, SiC nanowires were synthesized, taking advantage of the carbon source and 1D nanostructure of the carbonated BC template.[19] Three specific precursor strategies will be discussed in more detail below; electrospinning, atomic layer deposition (ALD), and layer-by-layer (LBL) deposition. Each is useful to exploit the fibrillar morphology while introducing precursors in a unique approach.

2.2.1. Electrospinning

Electrospinning utilizes an applied electric field to draw a charged solution into fibers, helping to form fibrillar CNFs and deposit potential precursors onto the surface.[40,41] This technique is commonly used to produce polymer filaments for textiles.[42] However, as a low cost, simple technique though, electrospinning has become a common technique to fabricate nanofibers for a range of applications.[43] The hydroxyl groups of cellulose allow for surface functionalization with charged groups including sulfates and phosphates, and the fibril structure of CNFs make the process of electrospinning easier. Likewise, the mechanical robustness and stability provide support for the final drawn fibers. Electrospun CNFs have been used to synthesize CFs.[20] The process of electrospinning produces aligned, uniform nanofibers, which after pyrolysis and activation, result in CFs. The performance of these CFs is tunable by varying the electrospinning conditions, providing a unique path to sustainably derived CFs. Another study used CNFs as a template to synthesize metal catalyst imbedded fibers.[21] CNFs were electrospun to form uniform fibers, surface polymerized with dopamine, and imbedded with silver nanoparticles. Final materials showed good electrical conductivity, mechanical strength, and adherence of the silver nanoparticles.

2.2.2. ALD

The ALD technique deposits an ultrathin, uniform film of precursor on a substrate sequentially using gas phase chemicals.[17] Precursors are first vaporized and released into a reactor to interact with a substrate one at a time. Specific amounts of precursor and interaction times allow for growth of desired film thickness. Any reaction byproducts and unreacted precursor molecules are removed, under ultrahigh vacuum, before introducing a subsequent precursor. ALD occurs at low temperature and can even coat complex structures, making it applicable for use with a range of templates. For cellulose nanofibers, ALD is commonly used to coat templated aerogels. Attributable to their mechanical strength and flexibility, these aerogels are stable even under the high vacuum conditions of ALD. The complex porosity in these aerogels produces a high surface area for functionalization, while the gas phase ALD reactions can fully saturate the surface. For example, a 7 nm thick TiO_2 film was coated on a CNF aerogel via ALD, creating photoswitchable superabsorbency.[22] In addition, nanoscale Al_2O_3 and ZnO can be attached to CNF aerogels to form functional materials for drug-release, catalyst, and microfluidic devices (**Figure 2**A).[17]

2.2.3. Layer-by-Layer Deposition

LBL deposition is another thin film fabrication technique to introduce precursors. During LBL, polyelectrolytes of opposite charges are deposited on a substrate alternatively in a simple, inexpensive, and rapid way.[44] Films produced by LBL process are very thin and contain controlled layered structures. As with other deposition techniques, templated cellulose nanofibers are useful when paired with LBL methodologies as they are mechanically robust enough to withstand the repeated layered process, while their porosity produces a substantial surface area for functionalization. In one study, CNFs were first coated with a ultrathin titania oxide layer via a repeated sol–gel process as shown in Figure 2B.[23] The CNF/TiO_2 hybrid film was then coated with an ultrathin chitosan (CS) layer in a similar fashion to obtain a CNF/TiO_2/CS hybrid composite. The layer thickness of TiO_2/CS composite coating was controlled by the deposition cycles. Finally, a layer of silver nitrate was attached to the hybrid composite surface and turned to Ag nanoparticles by an in situ reduction. In such a way, the biocidal effect of titania, the chelating ability of CS and antimicrobial Ag nanoparticles were combined for a stronger antibacterial performance. The CNF layer provided the necessary strong, functionable anchoring surface in both studies, which could support the final hybrid films.

2.3. Liquid Crystal Templates

Some of the pioneering work utilized cellulose nanomaterials as templates centered on the use of CNCs as liquid crystal templates.[5] An early study of Gray and co-workers discovered that CNCs formed a chiral nematic liquid crystal order in their colloid form above a threshold concentration.[45] Materials templated from the liquid crystal structures of CNCs achieve new interesting properties, such as high flexibility and strength.[39] The properties of the materials can be tuned by changing the CNCs' liquid crystal arrangement, making them potential materials for optoelectronics, biosensors, actuators, functional membranes, 3D printing, and tissue engineering.[6] However, for cellulose nanofibers, research on use of liquid crystal templates is ongoing. Kondo et al. have developed a strategy to align CNFs into nematic ordered cellulose (NOC).[24] This approach uses a system of dimethylacetamide/lithium chloride (DMAc/LiCl) to selectively swell cellulose fibers, causing realignment of the glucose rings. This results in availability of the hydroxyl group on carbon 6.[25] These aligned NOC structures display liquid crystal isotropy and are used to template other materials. The most common application for this technique is the templated growth of BC, although recent research has focused on ordered inorganic materials.[26,27]

© 2021 Wiley-VCH GmbH

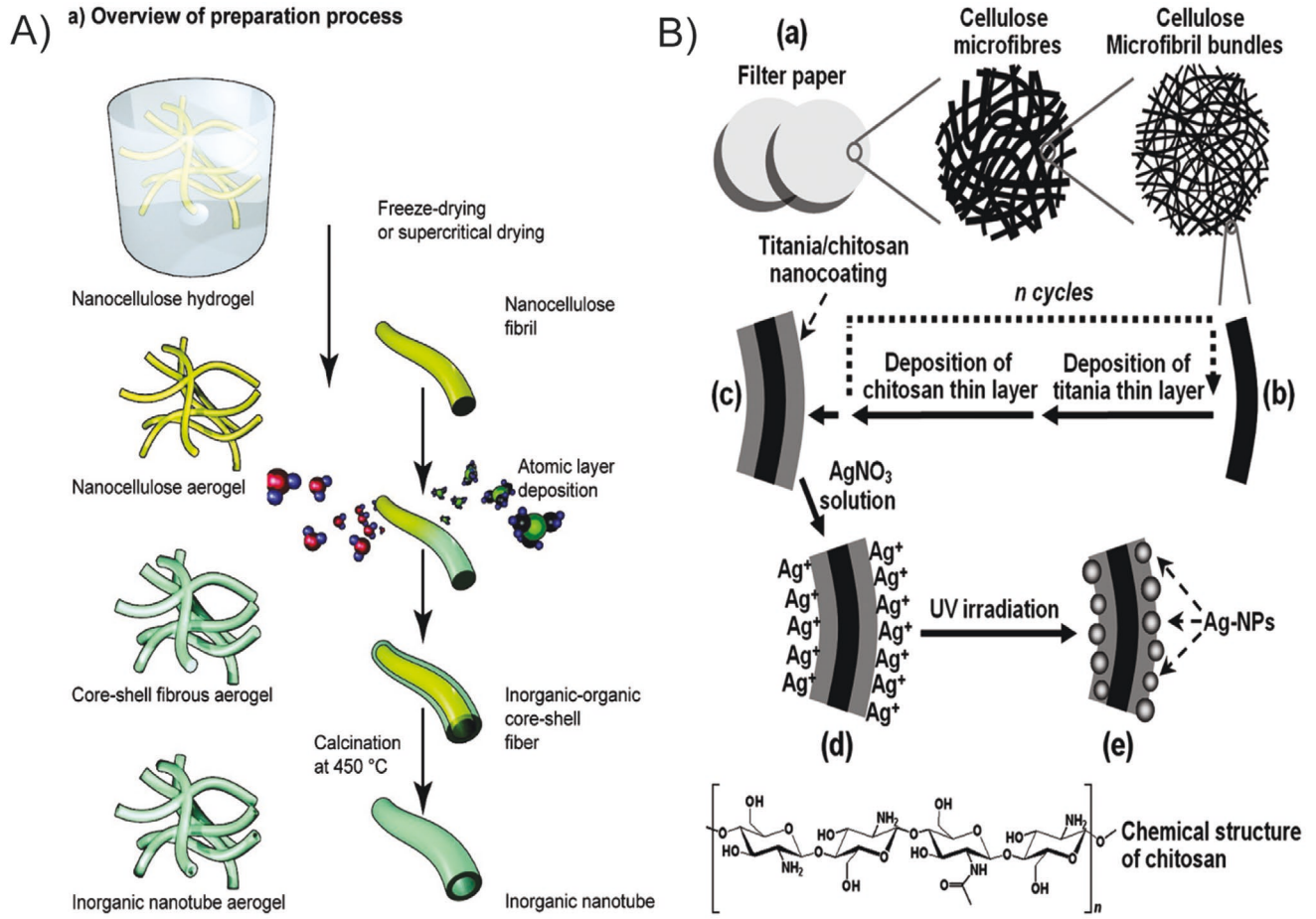

Figure 2. A) Schematic of fabricating inorganic nanotube via atomic layer deposition and CNF templating. Thermally controlled sacrificial templating is also utilized. Reproduced with permission.[17] Copyright 2011, American Chemical Society. B) Schematic illustration of the formation of CNF/titania/chitosan/Ag-NP composite film by layer-by-layer process. Reproduced with permission.[23] Copyright 2013, The Royal Society of Chemistry.

2.4. Co-Templating

Cellulose nanofibers have also been used in co-templating applications where they may be combined with other substances to form hybrid composite materials. Co-templates have improved properties compared to the properties of either template individually. Cellulose nanofibers are useful in co-templating applications as they can impart mechanical strength, hydrophilicity, and flexibility. These attributes make the co-templated material more stable and robust, resulting in overall property enhancement and easier synthesis. Without nanocellulose, many of these materials are simply too brittle or stiff and often undergo a loss in templating morphology during processing. In one case, co-templating might include blending the CNFs with polymers to form composites or with nanoparticles such as clays, graphene, and metal oxides to produce hybrid composites.[28] In another study, graphene oxide (GO) was co-templated with CNFs to form a precursor for a carbon network.[29] GO changed the morphology of carbonized CNFs from sphere to sheet. Meanwhile, carbonized CNFs reduced the number of defects in reduced GO as shown in **Figure 3**. The co-templated carbon network had excellent conductivity and can be used in lithium ion battery anodes for wearable electronics.

2.5. Sol–Gel

The sol–gel process is a method for producing solid materials from a solution of small molecules. This method is commonly used for the fabrication of inorganic oxides as shown in **Figure 4**.[30] The process typically starts with a hydrolysis of oxides to form hydroxides. The condensation among hydroxides produces oxo- or hydroxo-linkages, which forms colloids of solids dispersed in liquids (sol). Further condensation and removal of liquids, through various drying strategies, yield solids dispersed in a gas (gel).[30] Simply put, the sol–gel process converts a hydrogel to an aerogel.[31] Sol–gel processes most often occur in aqueous medium, making this method a convenient choice for use with cellulose nanofiber templating. Additionally, the hydrophilicity, water retention capability, and surface groups on cellulose nanofibers serve to assist in the sol–gel condensation process and help stabilize the resulting gel. Synthesized inorganic nanoparticles from nanocellulose

© 2021 Wiley-VCH GmbH

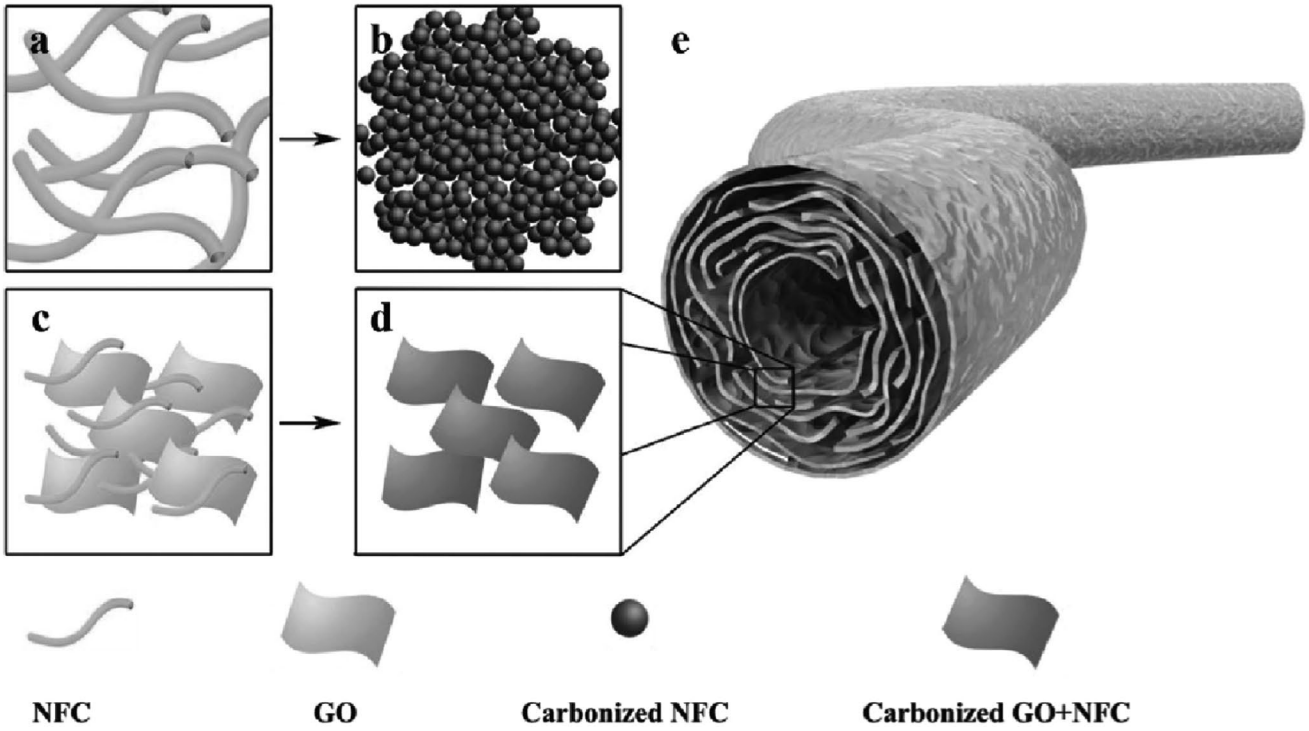

Figure 3. a,b) Fibril CNFs were changed to sphere particles after carbonization. c,d) Co-templating CNFs with GO maintained the fibril structure of CNFs after carbonization. e) Final morphology of the CNF–GO hybrid fibers after carbonization. a–e) Reproduced with permission.[29] Copyright 2014, Wiley-VCH.

templates via sol–gel process include gold, silica dioxide, calcium phosphates, tungsten oxide, among others.[15,26,32,33,34] Cellulose nanofibers are able to impart their porosity and a fibrillar structure on these templated materials, all of which can be retained after subsequent pyrolysis. This allows for production of unique morphologies including hollow tubes, dendrites, and a range of organic–inorganic core–shell structures.[15,17] The presence of these features and unique morphologies in the resultant materials provide enhancement in electrochemical and catalytic properties for many of their useful applications, as well as unique properties such as stimuli response useful in sensors.

2.6. Foaming

Nanocellulose foams and aerogels are another type of structural templates. In general, these materials encompass solid, liquid, and gel materials with an array of pore sizes ranging from microporous to mesoporous structures, all made with CNs.[35] These foams can be achieved by convective drying, freeze drying, or supercritical drying, allowing for tailored pore sizes and high porosity.[35] Foaming of CNFs is common practice and occurs during water removal even at low concentration fiber solutions. The fibril morphology, high water retention, mechanical strength, and abundance of surface hydroxyl groups of CNFs result in mechanically robust, stable, and self-standing foams capable of supporting and templating additional materials. Ferric and cobalt nanoparticles were synthesized on a freeze-dried BC aerogel. First, the aerogel was immersed in a $FeSO_4/CoCl_2$ solution at an elevated temperature for precipitating the metal hydroxides/oxides on to the aerogel. Then, the precursor was immersed in a reducing agent solution to yield a highly flexible magnetic aerogels.[36] A similar approach was applied to attach titanium dioxide (TiO_2) on a CNF aerogel.[37] Besides the liquid-phase reaction, nanoparticles can also be deposited on BC-aerogel templates via atomic layer deposition.[17,22]

3. Applications

Many references that employ cellulose nanofibers as templates, center on the benefits offered by the fibril structure, and its direct use in advanced functional material applications. The benefits of cellulose nanofibers specific to each application are discussed in the following, where they can be exploited toward properties specific to each application. These applications include easy formation of aerogels which produce high surface area and are useful for electrodes and separation membranes, abundant hydroxyl groups, which allow for functionalization with metals for catalysts, and high water retention capacity for building technologies like cement and insulating materials.[36,46] In this section, extensive discussion will occur regarding applications of cellulose nanofiber templated materials. The benefits of using cellulose nanofiber templating strategies compared with other strategies will also be examined. Advanced material applications include catalysts, energy

© 2021 Wiley-VCH GmbH

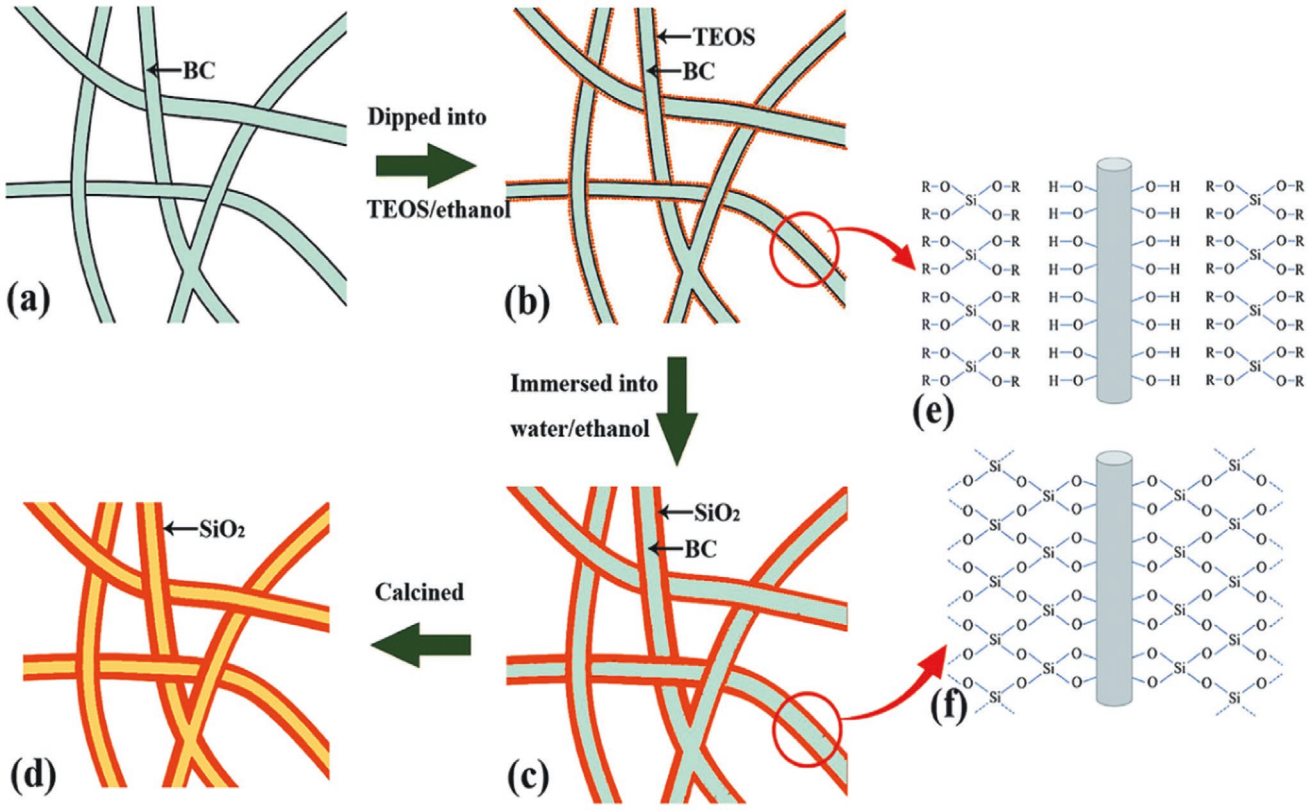

Figure 4. a–f) The synthesis route of silica nanotubes templated by BCs via a sol–gel process. (TEOS: tetraethyl orthosilicate). a–f) Reproduced with permission.[15] Copyright 2015, The Royal Society of Chemistry.

storage devices, building technology materials, biomedical devices, biomaterials, membranes, and separation materials (**Table 2**). These applications focus on using cellulose nanofiber templating to achieve unique, robust nanostructures. Additional applications of this type of templating, including packaging materials, textiles, and microfluidic devices, are arising every day.[36,47] Discussion of these applications will not be provided in this review due to limited availability of literature on these topics currently.

3.1. Catalysts

The unique structure and abundance of surface groups of CNFs make them a good template for the deposition of catalytic nanoparticles. First, the surface of these fibers can be readily modified, and the chemically modified surface groups can strongly anchor the metal species, promoting deposition of the catalysts on the surface of fibers. Second, specific morphologies of the catalysts can be obtained by taking advantage of the fibril structure. Moreover, the adequate chemical and structural stability of CNFs guarantee the reliability of nanocellulose-templated catalysts under different working environments. Catalysts with different morphologies can be obtained based on specific cellulose templates, e.g., CNFs, cellulose membranes, and cellulose foams.[48–51] Catalytic nanoparticles, including noble metals and metal oxides, can easily be synthesized and imbedded onto these surface of specific nanocellulose structures using cellulose nanofiber templates.

A BC membrane with a 3D porous network structure was directly used as a template for loading Cu_2O. These nanoparticle embedded foams showed a high specific catalytic activity for methylene blue degradation using hydrogen peroxide as oxidant.[49] The high surface area provided by the porous foam allowed for 100% degradation, while the embedded nanoparticles remained bound allowing for repeated cycling.

Similarly, BC was used to provide support for palladium (Pd) nanoparticles, and polyethyleneimine (PEI) was introduced to enhance the binding between BC and Pd. Overall, the cellulose framework provided mechanical strength, and improved the contact between the reactants and Pd nanoparticles because of its high porosity.[50] The Pd NPs were homogeneously dispersed on the surface of CNFs with a narrow size distribution (**Figure 5**A), which could be applied to heterogeneous Suzuki cross-coupling reaction between phenylboronic acid with iodobenzene, quickly achieving 100% yield in less than half an hour with high turnover frequency (TOF, >200 h^{-1}; Figure 5B,C). Moreover, attributable to the strong bond between the Pd and CNF surface, the catalyst could be easily separated from the reaction mixture and reused with high recyclability (Figure 5D).

Because of the insulating nature of nanocellulose materials, high-temperature pyrolysis of CNFs is necessary to make a conductive template or self-template for electrocatalyst. Pyrolytic

© 2021 Wiley-VCH GmbH

Table 2. List of examples from applications that use cellulose nanofiber templating.

Applications		Templating strategy	Starting materials	Final materials	Templating role of CNF	Outcomes (related to CNF properties)	Refs.
Catalyst		Precursor	BC, PEI, Pd nanoparticle precursors	Pd nanoparticle coated BC nanofibers	Support, sacrificial template, precursor	High catalytic activity, high turnover, mechanically robust	[50]
		Precursor-electrospinning	CNF, Ru particles, Ag particles	Metal particle coated CNF fibers	Support, fiber shape	Heterogenous, stable, reusable catalysts	[48]
Energy storage	Supercapacitors	Precursor	CNF, EDOT[a], iron salts	Poly (EDOT)[a] coated CNF	Support, fiber shape	Superior supercapacitor electrode performance[b]	[52]
		Precursor, foaming	CNF, RGO[c], CNT[d]	RGO/CNT imbedded CNF aerogel	Support, aerogel formation/shape		[53]
	Batteries	Co-templating, sacrificial templating	CNF, GO[e]	CNF–GO-based carbonized microfibers	Co-template, support, sacrificial template, precursor	Highly conductive, mechanically robust carbon microfibers with stable discharge	[29]
		Sol–gel, precursor-LBL	CNF paper, ITO[f] precursors	ITO[f] layered CNF paper	Support	Free-standing metal oxide films with high electrical conductivity	[54]
Building technology materials	Insulation and composite materials	Foaming, precursor	TEMPO[l]-CNF, GO[e], SEP[g], BA[h]	CNF–GO–BA–SEP foams	Support, foam formation/shape	Flexible, robust building foams with low thermal conductivity and good fire retardancy	[55]
	Cementitious composites	Precursor, sol–gel	TEMPO-CNF, cement[i]	CNF imbedded cement	Support	Strong, high thermal conductivity/CTE cement	[56]
Biomedical	Tissue scaffolding	Liquid crystal[j]	CNF film scaffold, human skin cells[k]	3D cell culture	Support	Mechanical stability, high water retention, reactive hydroxyl groups	[57]
Membranes and separation materials		Foaming, precursor-ALD	CNF, titania precursors	TiO_2 coated CNF aerogel	Support, aerogel formation/shape	Mechanically robust membrane with photoswitchable wetting properties	[22]

[a]EDOT: 3,4-ethylenedioxythiophene; [b]High electrode-normalized capacitances, volumetric energy, power densities, and excellent long-term stability; [c]RGO: reduced graphene oxide; [d]CNT: carbon nanotube; [e]GO: graphene oxide; [f]ITO: indium tin oxide; [g]SEP: sepiolite nanorods; [h]BA: boric acid; [i]Used cement is CEM I 32.5 N, produced in Bizert in a Tunisian plant, conforming to the Tunisian standard NT 47-01:198313 and the European standard EN 197-1:2000; [j]Liquid crystal technique is NOC: nematic ordered cellulose; [k]Human epidermal keratinocytes; [l]TEMPO: (2,2,6,6-tetramethylpiperidin-1-yl)oxyl oxidized.

treatment leads to the carbonization of cellulose nanofibers. Nanocellulose-derived carbon material itself is a good electrocatalyst for oxygen reduction reaction (ORR) and hydrogen evolution reaction (HER), with heteroatoms (B, N, P and S) doped during pyrolysis process to boost its electrocatalytic activity. A N-doped CNF aerogel was prepared by pyrolysis of BC and NH_3 activation, and possessed a high Brunauer–Emmett–Teller surface area and high N content, which showed superior ORR activity and electrochemical stability.[58] The use of cellulose-nanofiber-derived carbon-templated metal or metal oxide electrocatalysts are widely reported.[59] Generally, the metal ions are first absorbed on the surface of CNFs, then transformed into catalytic species via specific reactions like pyrolysis or calcination.

3.2. Electrochemical Energy Storage Devices

The high aspect ratio and exceptional mechanical properties of cellulose nanofibers make them a suitable substrate for freestanding and flexible electrodes and polymer electrolyte for use in electrochemical energy storage devices. Cellulose nanofibers also have good chemical and electrochemical stability, which guarantees their compatibility in most battery and supercapacitor systems with a wide working voltage range. Additionally, the abundant hydroxyl groups on the fiber surface can effectively regulate the ionic diffusion on the electrode/electrolyte interface, while the porous structure endows a large surface area, which is a desirable feature for high electrochemical performance of energy storage devices. Use of cellulose nanofibers in specific energy storage devices will be expanded on in subsequent sections.

3.2.1. Supercapacitors

Supercapacitors are promising energy storage devices with high power density, long cycle life, superior rate capability, simple principles, and low maintenance costs. Based on their working principles, supercapacitors are classified into three types: electrical double layer capacitors, which store energy by charge accumulation at the electrode/electrolyte interface; pseudo capacitors, which are based on fast redox reactions on the surface of electrodes for pseudocapacitance; and hybrid supercapacitors, which stores energy by combining both double layer capacitive and pseudocapacitive behaviors. Cellulose nanofiber templating can be used in supercapacitors via a few approaches. The fibers can serve as a cotemplate and integrate with active materials, undergo direct pyrolysis to carbon materials (active species), or be used to synthesize the separator membrane.

The highly porous structure of cellulose nanofibers are accepted as an ideal substrate for electrodes in supercapacitors. The large surface area is favorable for loading a large

© 2021 Wiley-VCH GmbH

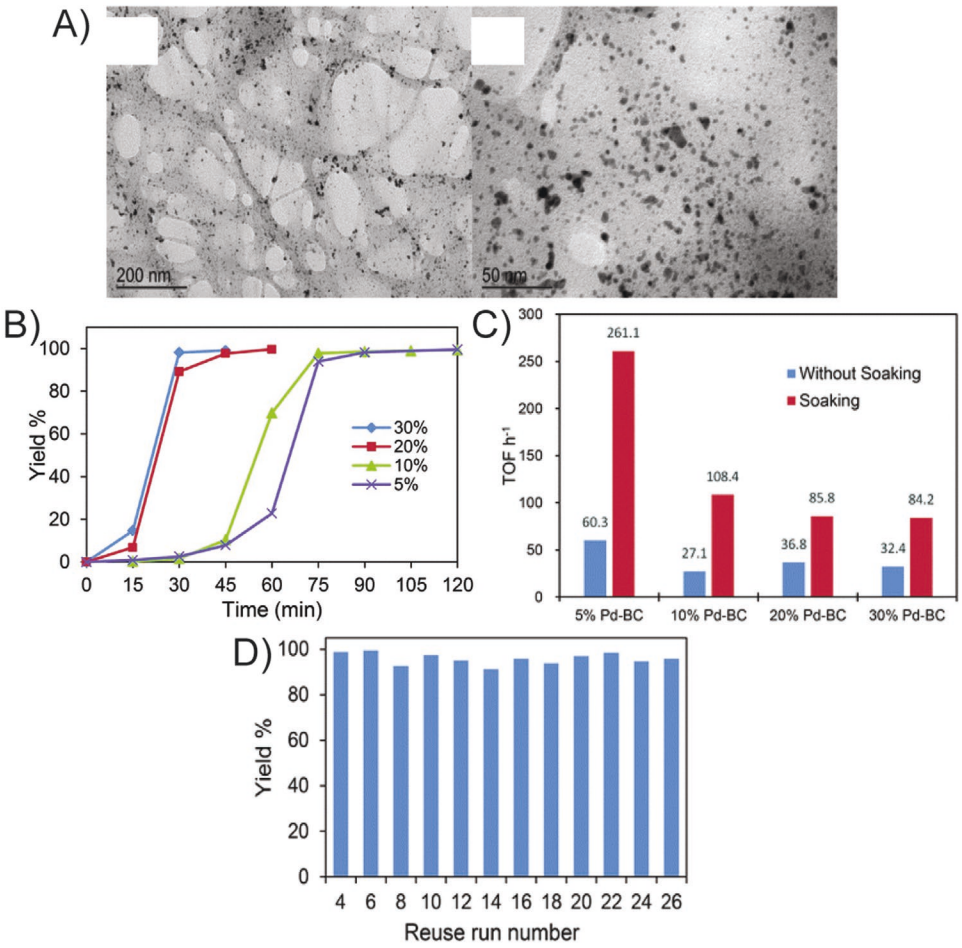

Figure 5. A) TEM images of Pd–BC. B) Yield of the Suzuki–Miyaura reaction of phenylboronic acid with iodobenzene in 95% ethanol using the catalytic sheet with different Pd–BC weight ratios; the catalytic sheet was soaked in water for 30 min before being used for the reaction. C) Turnover frequency (TOF) of the Suzuki–Miyaura reaction of phenylboronic acid with iodobenzene reaction. D) Yield obtained at 2 h reaction time in repeated runs of the Suzuki–Miyaura reaction of phenylboronic acid with iodobenzene. Reaction conditions: 1 mmol of iodobenzene, 1.1 mmol of phenylboronic acid, and 2 mmol of K_2CO_3; temperature = 80 °C. A–D) Reproduced with permission.[50] Copyright 2018, The Royal Society of Chemistry.

amount of conductive agent and active materials, which promotes the infiltration of electrolyte and provides more sites for charge storage. Moreover, nanocellulose-based electrodes possess high mechanical strength, which makes them easy to fabricate into flexible supercapacitors. Various active materials have been integrated into the cellulose nanofiber substrate, such as carbonaceous materials (e.g., CNTs, graphene, graphite, active carbon, and heteroatom-doped carbon), conductive polymers (e.g., polypyrrole, poly(3,4-ethylenedioxythiophene) (PEDOT), and polyaniline), and metal oxides (e.g., V_2O_5 and MnO_2).[52,60,61,62] Additionally, cellulose-nanofiber-based hybrid electrodes can be obtained via different approaches, including spinning, filtration, coating, and freeze-drying, which results in electrodes with different structures, such as fibers, films/membranes, and foams.[53,60,61,63] The loading of active materials will inevitably decrease the mechanical strength of the nanocellulose substrate, so it is necessary to optimize the balance between the mechanical properties and electrochemical performances of the hybrid electrodes for supercapacitors.

Niu et al. balanced the electrochemical properties and mechanical stability in their supercapacitor materials.[60] Cellulose nanofiber/single-walled carbon nanotube (CNF/SWCNT) hybrid nonwoven mats were synthesized using the CNF as a mat template (**Figure 6**A). These materials displayed a capacitance of about 5.99 mF cm^{-2} at a current density of 0.024 mA cm^{-2}, which is higher than traditional all-carbon materials. The porous structure of CNF is believed to be responsible for this increase in properties as it provides additional pathways for electrolyte diffusion. The CNF also imparted good mechanical stability, necessary for use as a potential wearable, without a loss in electrochemical performance, even after 5000 charge/discharge cycles. Repeated damage testing, where the mats were subjected to extreme deformations, resulted in no loss in capacitance retention (≈100%) or current density (Figure 6B–E).

CNFs are also an ideal template and precursor for porous carbon materials. The synthesized carbon materials (or carbon aerogel) possess many advantages, such as light weight, high specific surface area, and good electrical conductivity.

© 2021 Wiley-VCH GmbH

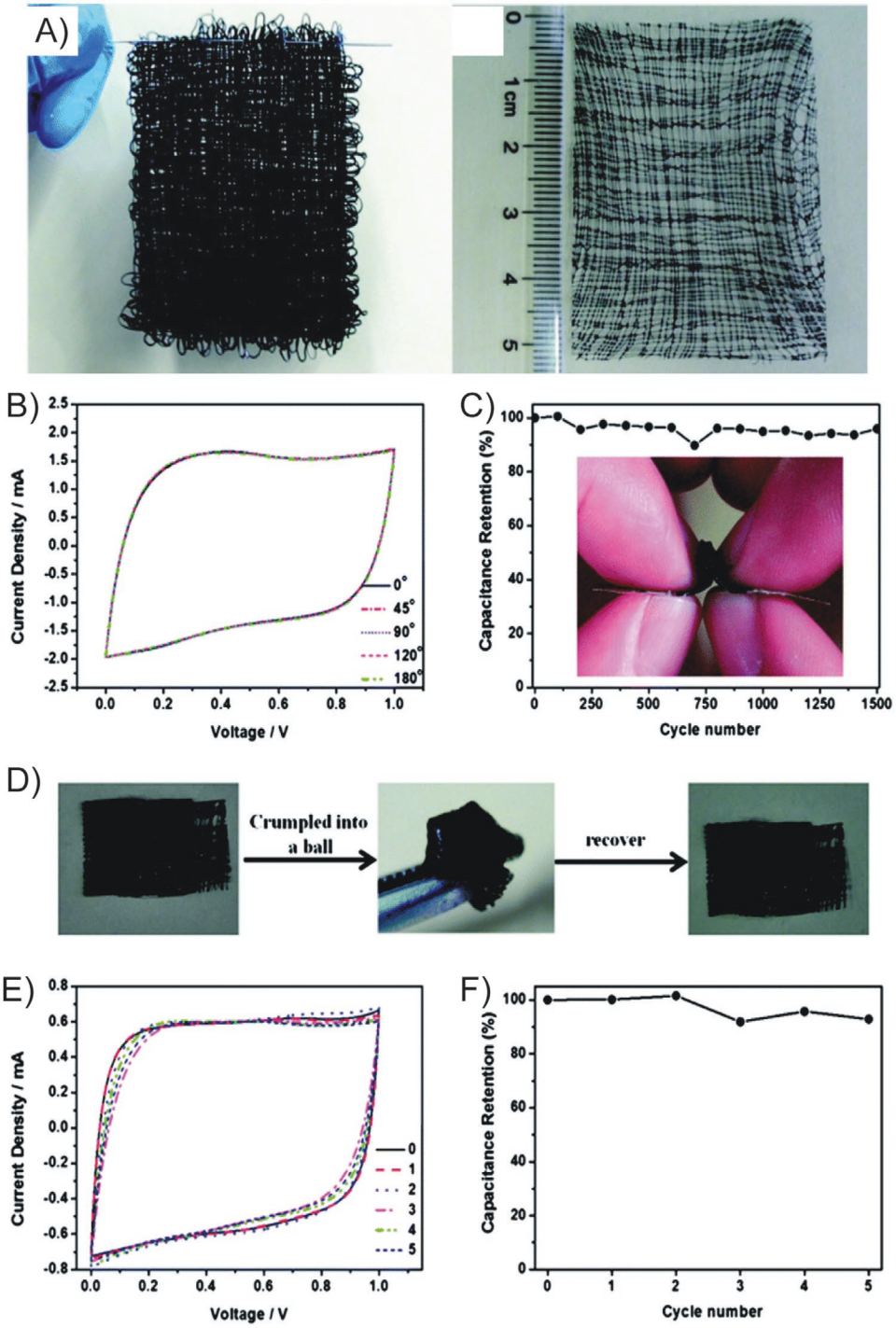

Figure 6. A) Photographs of the wet and dry CNF/SWCNT hybrid nonwoven mats. B) CV curves of the CNF/SWCNT mat wearable supercapacitors at different bending states of 0°, 45°, 90°, 120°, and 180° (50 mV s^{-1}). C) Durability test of the CNF/SWCNT mat wearable supercapacitor undergoing 1500 bending cycles according to CV curves at a scan rate of 50 mV s^{-1}. Inset: Photograph of the mat supercapacitor in a bending state (180°). D) Schematic illustration of extreme deformation. E) CV curves with the number of extreme deformation cycles at a scan rate of 50 mV s^{-1}. F) Normalized capacitance values versus the number of extreme deformation cycles. A–F) Reproduced with permission.[60] Copyright 2014, The Royal Society of Chemistry.

Cellulose-nanofiber-derived carbon materials can also be integrated in situ with other active materials, including other carbon materials, metal oxides, and sulfides, where the fiber acts as the template for the growth of active materials, and the conductive framework after pyrolysis.[18,64] Long et al. used BC nanofibers as a template to grow polyaniline, which was subsequently pyrolyzed and bound with MnO_2 to synthesize carbonized electrodes. These electrodes displayed good mechanical

© 2021 Wiley-VCH GmbH

stability due to the BC structure, with a high surface area for electrochemical reactions. When used as working electrodes in an aqueous Na_2SO_4 solution, these materials were able to reversibly charge/discharge at a voltage window of 2.0 V, while achieving an energy density of 63 Wh kg^{-1} and maximum power density of 227 kW kg^{-1}. These electrodes also maintained excellent cycling stability with 92% capacitance retention even after 5000 cycle. Overall, this example indicates that many of the promising properties of these carbon materials are not only beneficial for the electrochemical performance of supercapacitors but are a direct result of utilizing cellulose nanofibers.

3.2.2. Batteries

Batteries have a similar structure to supercapacitors, including the electrodes, separator, and electrolyte. In batteries though, there are two electrodes, which are named according to their electrochemical reaction types. An anode refers to the electrode where oxidation occurs, and the cathode refers to the electrode where reduction occurs. Batteries possess a much higher energy density than supercapacitors. In various battery systems (e.g., Li-ion batteries, Na-ion batteries, Zn-ion batteries, Li–S batteries, and Li–O_2 batteries) with different working principles, these fibers demonstrate their great application potential as a templating material.

Like the applications in supercapacitors, CNFs are used in batteries as a substrate to load both conductive agents and active materials. This fabrication method of cellulose nanofiber hybrid electrodes is also similar to those used for supercapacitors. Various cathode materials (e.g., $LiFePO_4$, $Li_4Ti_5O_{12}$, sulfur), anode materials (e.g., graphite, Si, SiO_2, TiO_2, SnO_2) and conductive agents (e.g., carbon black, CNTs) have been integrated with CN papers, produced from CNFs, to fabricate freestanding and flexible electrodes.[29,65,66] The mechanical stability and toughness of CNFs make fabrication possible.

Hu et al. who used a hybrid CNF–CF paper material to form porous networks, which were coated in silica using chemical deposition techniques.[66] The resulting aerogels were used as electrodes in lithium-ion batteries. The high porosity provided ample surface area for lithiation/delithiation during cycling (100 cycles), with little change in specific capacity (>1200 mAh g^{-1}). Additionally, silica is also known to increase in sizing during lithiation, so the flexibility in the electrodes, imparted by the CNF, is important to prevent damage during cycling. Overall, the performance of these templated electrodes was better than the theoretical capacity of graphite, a more traditional lithium battery electrode material.

Likewise, cellulose-nanofiber-derived carbon materials are also widely used to integrate with active materials for battery electrodes. The fibers act as a template for the deposition of precursors. During pyrolysis, the active materials (e.g., MoS_2, Fe_2O_3,) are in situ formed from the precursors on these nanocellulose-derived carbon framework.[67,68] The cellulose nanofibers serve as a sacrificial template in these methods, which can synthesize active materials with specific morphologies typically via calcination of cellulose nanofibers in air.[69] Wang et al. coated the surface of BC nanofibers with $SnCl_2$ particles.[68] These materials were then pyrolyzed to remove the cellulose and convert the precursor into active SnO_2 nanoparticles. The presence of cellulose nanofibers resulted in well dispersed tin oxide particles, which performed better during electrochemical testing. After 100 repeated cyclic testing, the BC immobilized tin obtained a specific capacity of ≈600 mAh g^{-1} under a current density of 100 mA g^{-1}, while nontemplated SnO_2 only obtained a specific capacity lower than 100 mAh g^{-1}. Similar experiments were performed with germanium nanoparticles, which also showed significant improvement in electrochemical properties in the BC nanofiber templating materials. This indicates the importance of utilizing a fibrillar-shaped template in these materials.

CNF membranes can also be used as a template for separators in batteries.[70] The porous structure, good mechanical properties, and high electrochemical and thermal stability help support templating for these applications.[71] The properties of a CNF separator can be tuned by the addition of inorganic oxide powders to improve the electrolyte uptake and the ionic conductivity.[72]

3.3. Building Technology Materials

3.3.1. Insulation and Composite Materials

The low density (≈5 kg m^{-3}) and coefficient of thermal expansion (CTE = 6 ppm K^{-1}) of nanocelluloses have been exploited for the design of cellulose-nanofiber-based foams and aerogels with superinsulation properties (i.e., materials of thermal conductivity below that of air, λ_{air} = 25 mW m^{-1} K^{-1}).[35,73] Foams and aerogels produced by either ice templating or supercritical CO_2 drying techniques have demonstrated characteristic low thermal conductivities (i.e., high thermal insulation) in the range of 15–30 mW m^{-1} K^{-1} because of the possibility of tuning the porous structure of the foams via process control, making them competitive with conventional insulation materials (**Table 3**).[74,75]

The thermal conductivity of porous solids is commonly approximated by the sum of four contributions: i) conduction through the solid, λ_s; ii) conduction through the gas, λ_g; iii) convection within the cells, λ_c; and iv) radiation through the cell walls and across the cell voids, λ_r.[80] Templating the nanocellulose foam and aerogel structure via ice templating (e.g., freeze-casting) and supercritical drying usually results in porous solids with cell sizes of below 10 mm, making the air convection within the cells negligible.[81] Solvent-exchange (from water to ethanol, in the case of supercritical drying) and directional freezing (control of the orientation of nanosized particles) are two key parameters that can be varied to decrease the pore size of nanocellulose foams in order to reduce the contribution of gas significantly and design super insulating materials. With a gaseous conductivity below 1 mW m^{-1} K^{-1} (estimated mean free path of the foams' cell walls of around 10 nm, against 70–75 nm in air), freeze-cast CNF-based foams, composed of sepiolite and graphene oxide, exhibited a radial thermal conductivity of around 18 mW m^{-1} K^{-1} (i.e., thermal conductivity measured parallel to the main orientation of the nanosized particles).[55,82] Varying the starting concentration

© 2021 Wiley-VCH GmbH

Table 3. Comparison of conventional insulation materials and CNF-based foams/aerogels.

Insulation materials	Bulk density [kg m^{-3}]	Thermal conductivity [mW m^{-1} K^{-1}]	Refs.
Calcium silicate	170–220	47	[76]
Cellular glass	130–160	55–58	
Mineral wool	100	35–44	
Glass wool	60	40	
XPS (extruded polystyrene)	45	≤29	
EPS (expanded polystyrene)	18	≤42	
PU foam	50	≤23	
CNFs (via mechanical treatment)	≈5	≈15	[77]
TEMPO-CNFs	≈5–6	≈15	
TEMPO-CNFs	7.5	15	[55]
TEMPO-CNFs/graphene oxide (10 wt%)/boric acid/sepiolite (10 wt%)	5.6	18	
TEMPO-CNFs/nanozeolites (2–10 wt%)	n/a	≤25	[78]
TEMPO-CNFs	17	18	[75]
TEMPO-CNFs (freeze-drying)	13–33	24–28	[79]
TEMPO-CNFs (spray freeze-drying)	12–30	18–21	

of the CNF gel can also alter the thermal conductivity of the resulting porous solids by acting on the solid's density and thus, the contribution of the solid phase. TEMPO-CNF aerogel densities varying from 17 to 37 mg cm^{-3} exhibited increased thermal conductivity values from 18 to 40 mW m^{-1} K^{-1}, respectively.[75] The thermal conductivities of these cellulose nanofiber templated materials are less than many traditional materials, as summarized in Table 3.

Selection of materials of high thermal boundary resistance or combination of nanosized components can also lower the solid phase contribution by enhancing the interfacial thermal resistance of the material, or Kapitza resistance, and therefore, reducing the phonon scattering effects.[55,78,83] For a bulk material of identical composition to the TEMPO-CNF/sepiolite/graphene oxide nanocomposite foams, the solid contribution was reduced from ≈1 to 0.04 W m^{-1} K^{-1}, respectively, by optimizing the components.[55] The porous network created by the orientation of cellulose nanofibrils upon freeze-casting contributed in carrying and entangling the sepiolite and graphene oxide particles. Unlike CNCs, the fibrillar entanglement of CNFs helps the design of self-standing foams from a low concentration suspension, and can be used as a template for further functionalization and/or post-treatments.[84,85] The radiative conductivity is generally found to increase with increasing cell size and to decrease with increasing relative density.[80] The foam geometry and material properties are critical factors for determining the radiative contribution to the overall heat transfer. To reduce the radiative part of the thermal conduction at any temperature, one may suggest the selection of materials for foams/aerogels that can strongly absorb infrared radiation such as carbonaceous materials.[83] For instance, the addition of 10% graphene oxide increased the mass attenuation coefficient in the mid-infrared range by 26% when added to TEMPO-CNF/sepiolite/graphene oxide-composite foams.[55] Modifying the properties of the starting CNF suspension such as solid content, colloidal stability (i.e., surface chemistry), and aspect ratio, is a straightforward strategy to enhance the thermal insulation properties of the resulting nanocellulose porous solid for use in energy-efficient building technology.[35,74,78] Careful selection of the foam-making process and control of processing parameters are also key to design superinsulating nanocellulose-based foams. We refer the readers to a few very recent review articles that discuss the influence of process parameters on the material properties.[35,85,86]

The nanocellulose porous solids, once templated, can be used as a template, preform or matrix for the design of advanced engineered materials, e.g., composites, for lightweight construction building technology. For instance, Nissilä et al. impregnated freeze-cast CNF aerogels with a bioepoxy resin via vacuum infusion process to increase the isotropic mechanical performance of the anisotropic porous solid and make it hydrophobic.[87] The Young's moduli of the epoxy/CNF foams increased to 3710 and 4420 MPa in the perpendicular and parallel directions, respectively, from a modulus of 2630 MPa for neat epoxy (at 35 °C).[87] Note that the compressive strength of the neat CNF foam was 7.5 and 20.9 kPa, in the perpendicular and parallel directions, respectively, at 40% strain. CNFs/polyvinyl alcohol (PVA) composite foams with improved mechanical performance were also prepared by directional ice templating, taking advantage of the morphological features of the fibrils to orient the PVA chains that were chemically crosslinked to the CNFs beforehand.[88] The anisotropic composite foams with clear tubular porous microchannels were further coated via silanization using a thermal chemical vapor deposition technique, which maintained the porous structure and morphology of the foams intact, and increased the density of foams by only 10%. An additional post-treatment was performed via vacuum-assisted liquid filling of the pores with a mixture of poly(dimethylsiloxane) (PDMS) and curing agent, that increased the mechanical performance of the foams by twofold compared to pure PDMS foams.[88] Such a post-treatment strategy allows the engineering of high-performance tailored materials that can be used for a large spectrum of applications.

© 2021 Wiley-VCH GmbH

3.3.2. Cementitious Composites

The improvement of cement properties through the addition of fibers such as steel, glass, or other synthetic fibers, has been in practice for decades. The use of cellulose nanofibers has demonstrated adequate bonding capacity to cement-based matrices for improvements in toughness, ductility, flexural capacity, and impact resistance.[89] More particularly, CNFs can be added to the cement mixture to template its porous structure. Porosity contributes to the lack of cement durability in wet and dry cycle aging, making cement more sensitive to the infiltration of water that induces precipitation of dissolved hydration products such as calcium hydroxide after evaporation, thus causing fiber mineralization. This effect is reduced when CNFs are added.[56] For instance, the addition of 1 wt% CNF into a bamboo fiber/cement composite improved and maintained the fiber-matrix bonding for 200 aging cycles, resulting in an increase in fracture toughness after aging.[90] The hydrophilic and hygroscopic nature of CNFs can also contribute to enhance the mechanical performance of cement. CNFs act as a "water reservoir," which accelerates the production of calcium silicate hydrate (CSH) gel during hydration of the fiber-cement composite structure, thus increasing physical bonding between the fibers and the matrix.[91] Use of cellulose nanofibers can help tune the hydration and porous structure of the cement mixture, thus altering its properties. Steric stabilization of cellulose nanofibers can increase the hydration process, similarly to the action of water reducing agents used to disperse cement particles.[92] The high surface area of cellulose nanofibers can act as nuclei to promote the nucleation of hydration product crystals at the early stages of the cement hardening, thus favoring accumulation and precipitation of hydrated products in the open pores, and reducing the porosity of the mixture.[56,89]

Cellulose nanofibers can regulate the microstructure of cement mixture, and in turn enhance the aging and mechanical performance of the composites. Several variables can be optimized for tailoring the properties of cementitious composites, such as cellulose nanofiber surface chemistry and morphology, the amount of cellulose nanofibers added to the mixture, and the process to incorporate them. For instance, the use of TEMPO-oxidized CNFs is expected to improve the water reservoir function of nanocellulose because of the presence of surface carboxyl groups, and thus to reduce the cement hydration process and autogenous shrinkage.[56] Aggregates of cellulose nanofibers can also retain larger amount of water, while cellulose nanofiber powder can entrap more air. An optimized dispersion of cellulose nanofibers in the cementitious matrix can reduce the large size porosity of the mixture.[92] For further details on the influence of cellulose nanofibers on the properties of cementitious composites, the reader is referred to a very recent review paper on the topic.[89]

3.4. Biomedical Devices and Biomaterials

The preparation of biomedical devices and biomaterials is an emerging field which exploits cellulose nanofiber templating.[14,93] Many biomaterials rely on specific morphologies and highly porous structures, requiring use of methodologies such as templating to achieve optimal results. Additionally, CNFs and BC nanofibers are biocompatible, making them optimal nonsacrificial scaffolds and templates for the development of many biomedical devices and biomaterials.

There are numerous applications for cellulose nanofiber templating, most of which exploit the inherent properties of the fibers. For example, the high-water retention and surface hydroxyl groups prove useful in the formation of structured antimicrobial polymer surfaces. CNFs were coordinated with copper (Cu^{2+}) and imbedded within a PVOH matrix to create randomly oriented fiber films, which underwent a slow release of Cu^{2+}.[94] The Cu^{2+} serves as an antimicrobial agent killing anything on the surface. These films show promise as a coating for biomedical devices which can suffer from surface fouling. The randomly aligned and coordinated CNFs in these materials is necessary for the controlled release of Cu^{2+} and the fibrillar geometry supports the overall mechanical stability of the film. Another application for cellulose nanofiber templating is drug delivery systems. Many synthetic drug delivery systems use nonsustainable polymers, some of which suffer from toxicity and poor stability. Comparatively, nanocellulose is sustainable, nontoxic, and has good mechanical stability. Zhao et al. used a PEI grafted CNF aerogel as a drug delivery vehicle for aspirin.[95] The high surface area of CNF and its reactive hydroxyl groups provide easy access and a high level of drug loading. The porosity also allowed for controlled release.

The other major biomaterials application for templating with cellulose nanofibers is used as a scaffold for tissue engineering.[38,96,97] Scaffolds are used to support new, growing cells for all different types of tissues. Scaffolds can be utilized in a lab environment to grow tissues and organs, or they can be placed internally and used to stabilize and support growth of tissues such as bone after an injury.[98] The microporous structure of CNF is ideal and allows for better cellular infiltration and vascularization.[99] Zhang et al. used electrospinning to align CNFs, which mimic the natural extracellular matrix in human bones.[100] Once aligned, the CNF template can then undergo infiltration with smaller molecules, including bone cells (osteocytes). The alignment of CNFs is necessary to create a microstructure, which can facilitate the development of healthy, strong bone. Attributable to its biocompatibility, these aligned CNF scaffolds can even be implanted and show recovery of the bone. There are a multitude of papers that utilize other templating strategies, including ice-templating, with CNFs toward engineering other tissues, which are not discussed in depth here but would be useful for the readers.[93,97,101]

3.5. Membranes and Separation Materials

Membranes and other separation materials rely on intricate nanostructures to selectively remove contaminates or sequester gases. One approach to achieve these detailed morphologies is with templating materials. The intrinsic porosity of cellulose nanofibers helps support the selective separation, while the mechanical robustness supports the overall membrane during the stress of use. BC–silica hybrid film was investigated using BC hydrogel as a soft template with tetraethyl orthosilicate (TEOS) as a precursor.[102] Hydrolysis of TEOS (absorbed on

© 2021 Wiley-VCH GmbH

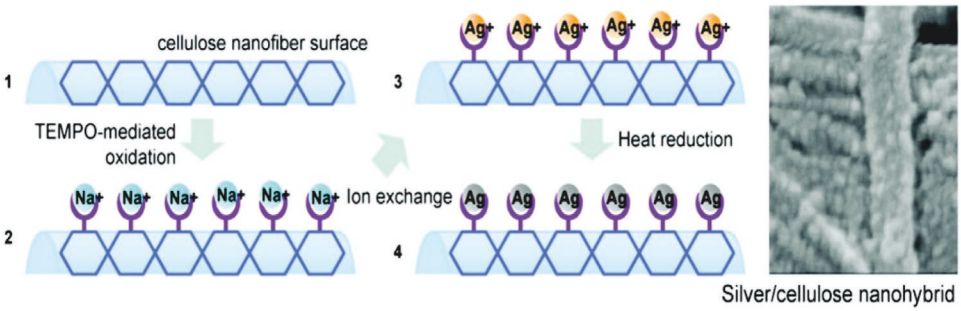

Figure 7. TEMPO-BC fiber templating Ag (silver) nanoparticles. Reproduced with permission.[104] Copyright 2009, American Chemical Society.

BC fiber surface) results in well dispersed silica sphere with 20–30 nm diameter in the BC–silica hybrid. Interestingly, the BC–silica hybrid has a broad and tunable emission band under UV excitation due to oxygen-related defects at the particle surface. Similarly, a BC–quantum dot (CdS) hybrid with well dispersed spherical CdS nanoparticles with 30 nm diameter was prepared in situ using $Cd(NO_3)_2 \cdot 5H_2O$ as the precursor and BC as the template.[103]

Ifuku et al. applied TEMPO-oxidized BC (TEMPO-BC) as a template to synthesize silver (Ag) nanoparticles on BC surface and form BC–Ag composites.[104] The procedure is illustrated in **Figure 7**, and includes TEMPO oxidation of BC, ion exchange from Na^+ to Ag^+, and further heating reduction to form Ag nanoparticles. TEMPO oxidation will bring carboxylate groups on to BC surface and can be used to quantitatively introduce guest metal ions by an ion-exchange reaction, and to further realize regular arrangement of salt. As a result, BC–Ag hybrids have well dispersed Ag nanoparticles and the particle size is tunable through adjusting the density of the carboxylate group in BC fiber.

Xiong et al. developed a CNF template guided assembly of silk fibroin (SF) into a peculiar "shish kebab" nanostructures on CNFs.[105] As shown in **Figure 8**, SFs are arranged periodically along the straight CNFs with average spacing of 17 ± 4 nm and height variation of 0.7 ± 0.2 nm, doubling the CNF diameter to around 4–5 nm and increasing the overall effective size. Authors also applied all-atom molecular dynamic simulations and revealed that modulated axial distribution of crystalline planes, hydrogen bonding, and hydrophobic interactions are the driving forces for this unique assembling behavior. Compared with other silk assemblies without CNFs, this strategy is a fast assembly process. The resultant CNF-SF membrane (50 nm thickness) demonstrates an extremely high flux, reaches to 3.5×104 L h^{-1} m^{-2} bar^{-1}, which is hundreds of times higher than commercial filtration membranes. Meanwhile, this membrane also has high reaction rates of 77% for rhodamine 6G and capability for capturing various heavy metal ions with high efficiency, demonstrating the potential applications in separations.

4. Conclusions and Outlook

4.1. Conclusions

As one of the most abundant natural resources, cellulose has been extensively investigated in material science to help produce advanced functional materials. Cellulose nanofiber templating has gained significant interest in recent years but remains as a newer technique with great potential still unrealized. The many promising properties inherent to cellulose nanofibers provide a framework to support properties in the final templated advanced materials. These templated materials will prove useful in a variety of applications including catalysis, energy storage, building technology, biomaterials, and separations.

Manufacturing of advanced functional materials via cellulose nanofiber templating involves pairing methodologies and materials, which can exploit properties inherent to cellulose that are useful in select applications. Sacrificial templating, aided by the ease in thermal removal of cellulose nanofiber templates, is promising in the creation of carbon materials for catalysis and energy storage. Meanwhile, simple foaming behavior, because of high water retention, and subsequent ease in aerogel formation, are promising for many advanced functional materials such as low density building technology materials, electrodes for energy storage, and porous membranes for separation. Additionally, methodologies that introduce surface coating strategies, such as ALD and LBL, are also beneficial in these examples. Likewise, the water-retention behavior of cellulose nanofibers in these templating strategies works in synergy with sol–gel processes to produce a range of stable materials. Moreover, biomedical advanced materials benefit from the biocompatibility and hydrophilicity of cellulose nanofibers. Overall, though, these materials all benefit from the mechanical stability and flexibility intrinsic to cellulose nanofibers, which allows for easier formation of robust materials. Therefore, careful selection of the materials and pairing them with the right cellulose nanofiber templating strategies can help enable the easier production of many of these advanced materials.

It is important to also compare cellulose nanofiber templating with other biomaterial templating strategies. Some other common biomaterials used in templating strategies include chitin and CNCs.[5,8,9,33,40,106–108] Currently, CNs are an excellent broad templating source derived from biomaterials for many applications. Chitin is a biopolymer comprising *N*-acetyl-D-glucosamine units.[109] In the literature, chitin templating is traditionally used for producing advanced biomaterials, but has recently shown promise with inorganic hybrids.[108,109] Further research is needed to push this templating strategy toward new applications.

© 2021 Wiley-VCH GmbH

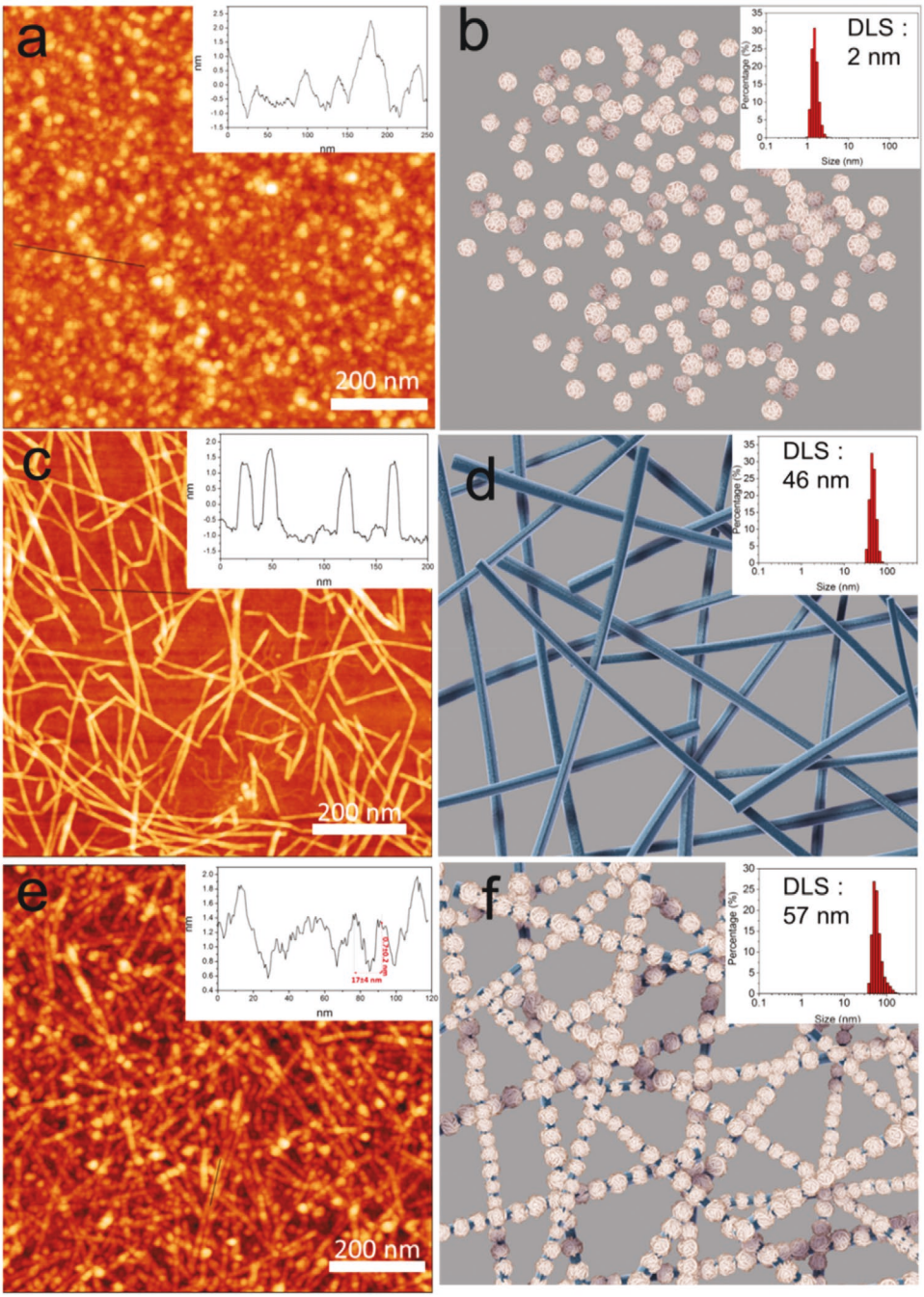

Figure 8. Morphologies of SFs, CNFs, and SF–CNFs assembly. a,c,e) Atomic force microscopy (AFM) topography images: a) SFs, c) CNFs, and e) assembled SF-30 wt% CNF materials (the insets in (a), (c), and (e) are the AFM cross-section profiles, *Z*-scale: 10 nm) with b,d,f) the corresponding schematics and DLS size distributions (insets): b) SFs, d) CNFs, and f) assembled SF-30 wt% CNF materials. a–f) Reproduced with permission.[105] Copyright 2017, American Chemical Society.

CNCs were introduced previously as a templating material. Cellulose nanofiber templating and CNC templating both feature many promising properties including surface hydroxyl groups for functionalization, high surface area, and overall hydrophilicity. These features allow for easier templating in solvents such as water, provide high templating efficiency, and can be easily adapted to template many systems. However, CNC templating has one unique feature which cellulose nanofiber templating cannot match. CNCs have the unique ability to self-assemble into a chiral nematic liquid crystalline phase, which can be transfer onto the templating material, allowing for production of templated, chiral ordered liquid crystal materials. Extensive literature has exploited this property to produce templated materials for advanced functional material applications.[5,6,8,34,106,110]

Cellulose nanofiber templating excels in a few application areas due to its unique features, as discussed earlier. The most

© 2021 Wiley-VCH GmbH

promising applications for cellulose nanofiber templating include those which rely on superior mechanical performance, both during the templating phase and present in the properties of the final material, and require formation of complex morphologies in the final materials. The high water retention and mechanical robustness of cellulose nanofibers allow templating to occur using a range of methodologies, even at high precursor loadings or under stressful conditions, without a collapse in template. Additionally, the long fibrillar morphology of cellulose nanofibers creates a strong, interconnect network of fibers which produce promising mechanical properties in the final materials, such as mechanical strength, toughness, and flexibility. Last, cellulose nanofiber templating can easily produce complex morphologies. Cellulose nanofibers easily undergo foaming to produce foams and aerogels, while the fibrillar structure of these nanofibers allows for stable formation of additional morphologies like hollow tubes and dendritic structures. Overall, when compared with other biomaterials, cellulose nanofiber templating is one of the most promising methods to produce advanced materials for applications with these specific requirements.

4.2. Outlook

Despite the promising progress in cellulose nanofiber templating, there are still some obstacles remaining for the further development and eventual commercialization of this templating strategy for many applications. Controlling the morphology of both the templating agent and final templated material is key to using templating strategies and remains a challenge for many templating techniques. In other words, how to customize the morphology of the templated materials and further tune their properties is still challenging. Current strategies on cellulose nanofiber templating are based on replication of the morphology of cellulose nanofibers or cellulose-nanofiber-based bulk materials. Unfortunately, the fundamental understanding of mechanism and relationship between cellulose nanofiber and templated materials is still lacking. Improved knowledge on how to control the morphology of the cellulose-nanofiber-based materials, e.g., gel, film, fibers, etc., can fuel future research on cellulose nanofiber templating and achieve tunability in the final products. Some studies have suggested that tunable morphologies could be achieved through the use of underdeveloped strategies like emulsions,[10,111] which could provide some insight for cellulose nanofiber templating. Meanwhile, the scale up of the cellulose-nanofiber-based templating processes for low cost production remains as a challenge. Despite the advantages of using nanocellulose, such as aqueous phase reactions, which result in efficient practices and can aid with cost and waste treatment, cellulose nanofibers are still more expensive than lower cost options like silica, which remains as a challenge. Development of lower cost methods to produce CNFs and BC nanofibers in the future will help assist in scalability of templating procedures and further enable this promising field.

Although challenges remain with cellulose nanofiber templating, we still would like to highlight some opportunities in this area. One direction is the use of cellulose nanofiber templating to produce ordered organic materials. Currently, cellulose-based templating is focused on use with inorganic materials, such as metal oxides. The thermal treatment to remove a cellulose nanofiber matrix in inorganic materials templating is not suitable for use with organic materials. Selective chemical removal of cellulose nanofibers after templating could be a potential solution. One possible approach is the removal of CNFs through dissolution using solvents, such as NaOH/urea, ionic liquids, and DMAc/LiCl.[112] Developments in this area and related strategies to effectively remove cellulose nanofibers from templated organic materials would provide new opportunities for both the cellulose nanofiber templating process and templated materials. Another direction for cellulose nanofiber templating involves the further development in methodology of this templating technique. Traditional templating strategies use aligned templates to impart morphologies in the final material. For example, nanopatterned silica wafers are a common template, which can be used to impart a specific morphology, using the nanopatterned surface, onto the templated material. Cellulose nanofiber templating is different because it exploits the properties inherent to these materials; fibrillar structure, aerogel formation; but does not use prealigned templates. Moving toward the use of preassembled cellulose nanofibers, where CNF or BC nanofibers are preferentially aligned as a template, would allow for further control of the morphology in templated materials. Currently, cellulose nanofiber alignment is quite difficult and needs further development to produce more facile strategies. Development of new cellulose nanofiber alignment techniques will benefit templating as well, including further research into top-down strategies, which exploit aligned cellulose present in natural sources like wood.[113] Other new methodologies can also be promising for cellulose nanofiber templating.

As a concluding remark, we believe cellulose-nanofiber-based templating for fabrication of advanced functional materials is a growing area of research. Unique attributes of these nanoscale fibers enable utilization of a variety of templating mechanisms and methodologies to create controlled morphologies, useful in an array of applications. The distinctive properties of CNFs and BCs enable formation of a wide range of advanced materials as discussed in the review. Researchers have just begun to explore the potential applications for advanced materials using CNF templating. New strategy development and further fundamental understanding will provide the next steps for continued research into this promising new area.

Acknowledgements

This research was supported by the US Department of Energy (DOE), Office of Energy Efficiency and Renewable Energy, Advanced Manufacturing Office, under contract DE-AC05-00OR22725 with UT-Battelle LLC and used resources at the Manufacturing Demonstration Facility at Oak Ridge National Laboratory, a User Facility of DOE's Office of Energy Efficiency and Renewable Energy. A.J.R. research was sponsored by the Laboratory Directed Research and Development Program of Oak Ridge National Laboratory (ORNL), managed by UT-Battelle, LLC for the U. S. Department of Energy under Contract No. De-AC05-00OR22725. Authors from the University of Maine are grateful for the funding support from UT-Battelle LLC with the US DOE under contract DE-AC05-00OR22725 (subcontract # 4000174848). T.L. and L.H. acknowledge the support of the US National Science Foundation (Grant Nos.: 1362256 and 1936452).

© 2021 Wiley-VCH GmbH

Conflict of Interest

The authors declare no conflict of interest.

Keywords

bacterial cellulose, cellulose nanofibers, cellulose nanofibrils, cellulose templating, functional materials

Received: August 14, 2020
Revised: October 5, 2020
Published online: February 9, 2021

[1] a) F. Cheng, J. Liang, Z. Tao, J. Chen, *Adv. Mater.* **2011**, *23*, 1695; b) T. G. Kim, H. Shin, D. W. Lim, *Adv. Funct. Mater.* **2012**, *22*, 2446; c) M. Ulbricht, *Polymer* **2006**, *47*, 2217.

[2] a) D. Klemm, F. Kramer, S. Moritz, T. Lindstrom, M. Ankerfors, D. Gray, A. Dorris, *Angew. Chem., Int. Ed.* **2011**, *50*, 5438; b) R. J. Moon, A. Martini, J. Nairn, J. Simonsen, J. Youngblood, *Chem. Soc. Rev.* **2011**, *40*, 3941; c) K. Li, L. N. Skolrood, T. Aytug, H. Tekinalp, S. Ozcan, *ACS Sustainable Chem. Eng.* **2019**, *7*, 14341; d) S. Sinquefield, P. N. Ciesielski, K. Li, D. J. Gardner, S. Ozcan, *ACS Sustainable Chem. Eng.* **2020**, *8*, 9601.

[3] B. Thomas, M. C. Raj, A. K. B, R. M. H, J. Joy, A. Moores, G. L. Drisko, C. Sanchez, *Chem. Rev.* **2018**, *118*, 11575.

[4] T. Abitbol, A. Rivkin, Y. Cao, Y. Nevo, E. Abraham, T. Ben-Shalom, S. Lapidot, O. Shoseyov, *Curr. Opin. Biotechnol.* **2016**, *39*, 76.

[5] a) M. Giese, L. K. Blusch, M. K. Khan, M. J. MacLachlan, *Angew. Chem., Int. Ed.* **2015**, *54*, 2888; b) G. R. Meseck, A. S. Terpstra, M. J. MacLachlan, *Curr. Opin. Colloid Interface Sci.* **2017**, *29*, 9.

[6] W. Y. Hamad, in *Cellulose Chemistry and Properties: Fibers, Nanocelluloses and Advanced Materials* (Ed: O. J. Rojas), Springer International Publishing, Cham, Switzerland **2016**, p. 287.

[7] a) N. Lin, J. Huang, A. Dufresne, *Nanoscale* **2012**, *4*, 3274; b) K. E. Shopsowitz, J. A. Kelly, W. Y. Hamad, M. J. MacLachlan, *Adv. Funct. Mater.* **2014**, *24*, 327; c) M. Morits, V. Hynninen, A. N. Nonappa, O. Ikkala, A. H. Groschel, M. Mullner, *Polym. Chem.* **2018**, *9*, 1650; d) B. L. Tardy, B. D. Mattos, L. G. Greca, T. Kamarainen, K. W. Klockars, O. J. Rojas, *Adv. Funct. Mater.* **2019**, *29*, 1808518; e) P. X. Wang, W. Y. Hamad, M. J. MacLachlan, *Angew. Chem., Int. Ed.* **2016**, *55*, 12460; f) Y. H. Yoon, S. Y. Lee, J. G. Gwon, H. J. Cho, Q. Wu, Y. H. Kim, W. H. Lee, *Ceram. Int.* **2018**, *44*, 16647; g) P. Dhar, S. S. Gaur, A. Kumar, V. Katiyar, *Sci. Rep.* **2018**, *8*, 3886; h) A. Ivanova, B. Frka-Petesic, A. Paul, T. Wagner, A. N. Jumabekov, Y. Vilk, J. Weber, J. Schmedt Auf der Gunne, S. Vignolini, M. Tiemann, D. Fattakhova-Rohlfing, T. Bein, *ACS Appl. Mater. Interfaces* **2020**, *12*, 12639; i) Y. Shin, G. J. Exarhos, *Mater. Lett.* **2007**, *61*, 2594; j) X. Y. Wu, Z. Q. Shi, R. Tjandra, A. J. Cousins, S. Sy, A. P. Yu, R. M. Berry, K. C. Tam, *J. Mater. Chem. A* **2015**, *3*, 23768; k) Y. T. Xu, Y. Dai, T. D. Nguyen, W. Y. Hamad, M. J. MacLachlan, *Nanoscale* **2018**, *10*, 3805; l) Y. H. Yoon, S. Y. Lee, J. G. Gwon, H. J. Cho, Q. Wu, W. H. Lee, *Cellulose* **2018**, *25*, 6591; m) S. Z. Zhang, W. He, X. D. Zhang, G. H. Yang, J. Y. Ma, X. N. Yang, X. Song, *Electrochim. Acta* **2015**, *174*, 1175; n) X. D. Zheng, Y. Y. Wang, F. X. Qiu, Z. Y. Li, Y. S. Yan, *J. Chem. Eng. Data* **2019**, *64*, 926; o) Y. Lu, A. A. Armentrout, J. C. Li, H. L. Tekinalp, J. Nanda, S. Ozcan, *J. Mater. Chem. A* **2015**, *3*, 13350.

[8] M. Giese, M. Spengler, *Mol. Syst. Des. Eng.* **2019**, *4*, 29.

[9] M. L. Hassan, S. M. Fadel, C. Moorefield, G. R. Newkome, *J. Macromol. Sci., Part A: Pure Appl.Chem.* **2014**, *51*, 743.

[10] Y. Lu, J. E. Poole, T. Aytug, H. M. Meyer, S. Ozcana, *RSC Adv.* **2015**, *5*, 103680.

[11] a) M. T. P. da Silva, J. C. Carvalho, S. B. C. Pergher, T. P. Braga, *J. Porous Mater.* **2016**, *23*, 811; b) F. Hasanpour, M. Taei, S. H. Banitaba, M. Heidari, *Mater. Sci. Eng., C* **2017**, *76*, 88; c) M. A. Mohamed, W. N. W. Salleh, J. Jaafar, Z. A. Mohd Hir, M. S. Rosmi, M. Abd Mutalib, A. F. Ismail, M. Tanemura, *Carbohydr. Polym.* **2016**, *146*, 166; d) F. RenChun, D. Jun, H. Hui, G. Zhong-Cheng, *High Perform. Polym.* **2014**, *26*, 27.

[12] E. Kontturi, P. Laaksonen, M. B. Linder, A. H. G. Nonappa, O. J. Rojas, O. Ikkala, *Adv. Mater.* **2018**, *30*, 1703779.

[13] a) J. Huang, T. Kunitake, *J. Am. Chem. Soc.* **2003**, *125*, 11834; b) S. Chen, B. Zhou, W. Hu, W. Zhang, N. Yin, H. Wang, *Carbohydr. Polym.* **2013**, *92*, 1953; c) M. Kaushik, A. Moores, *Green Chem.* **2016**, *18*, 622.

[14] Y. Xue, Z. Mou, H. Xiao, *Nanoscale* **2017**, *9*, 14758.

[15] Y. Z. Wan, Z. W. Yang, G. Y. Xiong, S. R. Raman, H. L. Luo, *RSC Adv.* **2015**, *5*, 48875.

[16] S. Li, Y. M. Zhang, J. G. Huang, *J. Alloys Compd.* **2019**, *783*, 793.

[17] J. T. Korhonen, P. Hiekkataipale, J. Malm, M. Karppinen, O. Ikkala, R. H. Ras, *ACS Nano* **2011**, *5*, 1967.

[18] C. L. Long, D. P. Qi, T. Wei, J. Yan, L. L. Jiang, Z. J. Fan, *Adv. Funct. Mater.* **2014**, *24*, 3953.

[19] L. X. Wen, Y. J. Ma, B. Dai, Y. Zhou, J. S. Liu, C. H. Pei, *Mater. Res. Bull.* **2013**, *48*, 687.

[20] L. B. Deng, R. J. Young, I. A. Kinloch, Y. Q. Zhu, S. J. Eichhorn, *Carbon* **2013**, *58*, 66.

[21] H. Gaminian, M. Montazer, *Cellulose* **2017**, *24*, 3179.

[22] M. Kettunen, R. J. Silvennoinen, N. Houbenov, A. Nykanen, J. Ruokolainen, J. Sainio, V. Pore, M. Kemell, M. Ankerfors, T. Lindstrom, M. Ritala, R. H. A. Ras, O. Ikkala, *Adv. Funct. Mater.* **2011**, *21*, 510.

[23] W. Xiao, J. Xu, X. Liu, Q. Hu, J. Huang, *J. Mater. Chem. B* **2013**, *1*, 3477.

[24] T. Kondo, E. Togawa, R. M. Brown Jr., *Biomacromolecules* **2001**, *2*, 1324.

[25] E. Togawa, T. Kondo, *J. Polym. Sci., Part B: Polym. Phys.* **1999**, *37*, 451.

[26] K. Higashi, T. Kondo, *Cellulose* **2012**, *19*, 81.

[27] a) T. Kondo, W. Kasai, M. Nojiri, Y. Hishikawa, E. Togawa, D. Romanovicz, R. M. Brown Jr., *J. Biosci. Bioeng.* **2012**, *114*, 113; b) T. Kondo, M. Nojiri, Y. Hishikawa, E. Togawa, D. Romanovicz, R. M. Brown Jr., *Proc. Natl. Acad. Sci. USA* **2002**, *99*, 14008.

[28] a) H. P. S. Abdul Khalil, A. H. Bhat, A. F. Ireana Yusra, *Carbohydr. Polym.* **2012**, *87*, 963; b) R. Bardet, C. Reverdy, N. Belgacem, I. Leirset, K. Syverud, M. Bardet, J. Bras, *Cellulose* **2015**, *22*, 1227.

[29] Y. Y. Li, H. L. Zhu, F. Shen, J. Y. Wan, X. G. Han, J. Q. Dai, H. Q. Dai, L. B. Hu, *Adv. Funct. Mater.* **2014**, *24*, 7366.

[30] N. D. Petkovich, A. Stein, *Chem. Soc. Rev.* **2013**, *42*, 3721.

[31] H. Kargarzadeh, J. Huang, N. Lin, I. Ahmad, M. Mariano, A. Dufresne, S. Thomas, A. Galeski, *Prog. Polym. Sci.* **2018**, *87*, 197.

[32] a) T. J. Zhang, W. Wang, D. Y. Zhang, X. X. Zhang, Y. R. Ma, Y. L. Zhou, L. M. Qi, *Adv. Funct. Mater.* **2010**, *20*, 1152; b) J. A. Kelly, M. Yu, W. Y. Hamad, M. J. MacLachlan, *Adv. Opt. Mater.* **2013**, *1*, 295; c) F. Chai, R. X. Tan, F. H. Cao, F. Y. Zhai, X. H. Wang, C. L. Shao, Y. C. Liu, *Mater. Lett.* **2007**, *61*, 3939.

[33] E. Dujardin, M. Blaseby, S. Mann, *J. Mater. Chem.* **2003**, *13*, 696.

[34] K. E. Shopsowitz, H. Qi, W. Y. Hamad, M. J. Maclachlan, *Nature* **2010**, *468*, 422.

[35] N. Lavoine, L. Bergstrom, *J. Mater. Chem. A* **2017**, *5*, 16105.

[36] R. T. Olsson, M. A. Azizi Samir, G. Salazar-Alvarez, L. Belova, V. Strom, L. A. Berglund, O. Ikkala, J. Nogues, U. W. Gedde, *Nat. Nanotechnol.* **2010**, *5*, 584.

[37] A. Henry, S. Plumejeau, L. Heux, N. Louvain, L. Monconduit, L. Stievano, B. Boury, *ACS Appl. Mater. Interfaces* **2015**, *7*, 14584.

[38] J. G. Torres-Rendon, T. Femmer, L. De Laporte, T. Tigges, K. Rahimi, F. Gremse, S. Zafarnia, W. Lederle, S. Ifuku, M. Wessling, *Adv. Mater.* **2015**, *27*, 2989.

© 2021 Wiley-VCH GmbH

[39] M. K. Khan, W. Y. Hamad, M. J. Maclachlan, *Adv. Mater.* **2014**, *26*, 2323.
[40] K. De France, Z. Zeng, T. Wu, G. Nystrom, *Adv. Mater.*, https://doi.org/adma.202000657.
[41] J. Xue, T. Wu, Y. Dai, Y. Xia, *Chem. Rev.* **2019**, *119*, 5298.
[42] a) M. Bognitzki, W. Czado, T. Frese, A. Schaper, M. Hellwig, M. Steinhart, A. Greiner, J. H. Wendorff, *Adv. Mater.* **2001**, *13*, 70; b) D. Zhang, *Advances in Filament Yarn Spinning of Textiles and Polymers*, Elsevier Science, Amsterdam, The Netherlands **2014**.
[43] V. Thavasi, G. Singh, S. Ramakrishna, *Energy Environ. Sci.* **2008**, *1*, 205.
[44] K. Ariga, Y. Yamauchi, G. Rydzek, Q. M. Ji, Y. Yonamine, K. C. W. Wu, J. P. Hill, *Chem. Lett.* **2014**, *43*, 36.
[45] J. F. Revol, H. Bradford, J. Giasson, R. H. Marchessault, D. G. Gray, *Int. J. Biol. Macromol.* **1992**, *14*, 170.
[46] Q. Zhang, L. Zhang, W. Wu, H. Xiao, *Carbohydr. Polym.* **2020**, *229*, 115454.
[47] a) A. Eivazihollagh, J. Backstrom, C. Dahlstrom, F. Carlsson, I. Ibrahem, B. Lindman, H. Edlund, M. Norgren, *Mater. Lett.* **2017**, *187*, 170; b) V. Thiruvengadam, S. Vitta, *J. Appl. Phys.* **2016**, *119*, 244312.
[48] M. Gopiraman, H. Bang, G. Yuan, C. Yin, K. H. Song, J. S. Lee, I. M. Chung, R. Karvembu, I. S. Kim, *Carbohydr. Polym.* **2015**, *132*, 554.
[49] G. G. Liu, F. He, X. Q. Li, S. H. Wang, L. J. Li, G. F. Zuo, Y. Huang, Y. Z. Wan, *J. Mater. Chem.* **2011**, *21*, 10637.
[50] Z. Y. Xiang, Y. Chen, Q. G. Liu, F. C. Lu, *Green Chem.* **2018**, *20*, 1085.
[51] Y. Li, L. Xu, B. Xu, Z. Mao, H. Xu, Y. Zhong, L. Zhang, B. Wang, X. Sui, *ACS Appl. Mater. Interfaces* **2017**, *9*, 17155.
[52] Z. H. Wang, P. Tammela, J. X. Huo, P. Zhang, M. Stromme, L. Nyholm, *J. Mater. Chem. A* **2016**, *4*, 1714.
[53] Q. Zheng, Z. Cai, Z. Ma, S. Gong, *ACS Appl. Mater. Interfaces* **2015**, *7*, 3263.
[54] Y. Aoki, J. G. Huang, T. Kunitake, *J. Mater. Chem.* **2006**, *16*, 292.
[55] B. Wicklein, A. Kocjan, G. Salazar-Alvarez, F. Carosio, G. Camino, M. Antonietti, L. Bergstrom, *Nat. Nanotechnol.* **2015**, *10*, 277.
[56] R. Mejdoub, H. Hammi, J. J. Sunol, M. Khitouni, A. M'nif, S. Boufi, *J. Compos. Mater.* **2017**, *51*, 2491.
[57] T. Seyama, E. Y. Suh, T. Kondo, *Biofabrication* **2013**, *5*, 025010.
[58] H. W. Liang, Z. Y. Wu, L. F. Chen, C. Li, S. H. Yu, *Nano Energy* **2015**, *11*, 366.
[59] a) S. S. Liu, W. N. Yan, X. C. Cao, Z. F. Zhou, R. Z. Yang, *Int. J. Hydrogen Energy* **2016**, *41*, 5351; b) F. Lai, Y. E. Miao, Y. Huang, Y. Zhang, T. Liu, *ACS Appl. Mater. Interfaces* **2016**, *8*, 3558.
[60] Q. Niu, K. Gao, Z. Shao, *Nanoscale* **2014**, *6*, 4083.
[61] a) Y. Liu, J. Zhou, E. W. Zhu, J. Tang, X. H. Liu, W. H. Tang, *J. Mater. Chem. C* **2015**, *3*, 1011; b) K. H. Choi, J. Yoo, C. K. Lee, S. Y. Lee, *Energy Environ. Sci.* **2016**, *9*, 2812.
[62] a) A. Razaq, L. Nyholm, M. Sjodin, M. Stromme, A. Mihranyan, *Adv. Energy Mater.* **2012**, *2*, 445; b) H. H. Wang, E. W. Zhu, J. Z. Yang, P. P. Zhou, D. P. Sun, W. H. Tang, *J. Phys. Chem. C* **2012**, *116*, 13013.
[63] L. Hu, J. W. Choi, Y. Yang, S. Jeong, F. La Mantia, L. F. Cui, Y. Cui, *Proc. Natl. Acad. Sci. USA* **2009**, *106*, 21490.
[64] a) L. F. Chen, Z. H. Huang, H. W. Liang, Q. F. Guan, S. H. Yu, *Adv. Mater.* **2013**, *25*, 4746; b) F. Lai, Y. E. Miao, L. Zuo, H. Lu, Y. Huang, T. Liu, *Small* **2016**, *12*, 3235.
[65] a) S. Leijonmarck, A. Cornell, G. Lindbergh, L. Wagberg, *Nano Energy* **2013**, *2*, 794; b) M. P. Yu, J. S. Ma, M. Xie, H. Q. Song, F. Y. Tian, S. S. Xu, Y. Zhou, B. Li, D. Wu, H. Qiu, R. M. Wang, *Adv Energy Mater* **2017**, *7*, 1602347.
[66] L. B. Hu, N. Liu, M. Eskilsson, G. Y. Zheng, J. McDonough, L. Wagberg, Y. Cui, *Nano Energy* **2013**, *2*, 138.
[67] a) F. Zhang, Y. B. Tang, Y. Yang, X. L. Zhang, C. S. Lee, *Electrochim. Acta* **2016**, *211*, 404; b) Y. Huang, Z. X. Lin, M. B. Zheng, T. H. Wang, J. Z. Yang, F. S. Yuan, X. Y. Lu, L. Liu, D. P. Sun, *J. Power Sources* **2016**, *307*, 649.
[68] B. Wang, X. Li, B. Luo, J. Yang, X. Wang, Q. Song, S. Chen, L. Zhi, *Small* **2013**, *9*, 2399.
[69] a) H. Guo, R. Mao, X. J. Yang, J. Chen, *Electrochim. Acta* **2012**, *74*, 271; b) Y. M. Sun, X. L. Hu, J. C. Yu, Q. Li, W. Luo, L. X. Yuan, W. X. Zhang, Y. H. Huang, *Energy Environ. Sci.* **2011**, *4*, 2870.
[70] a) F. Colò, F. Bella, J. R. Nair, M. Destro, C. Gerbaldi, *Electrochim. Acta* **2015**, *174*, 185; b) M. X. Li, X. W. Wang, Y. Q. Yang, Z. Chang, Y. P. Wu, R. Holze, *J. Membr. Sci.* **2015**, *476*, 112; c) Z. D. Gordon, T. Yang, G. B. G. Morgado, C. K. Chan, *ACS Sustainable Chem. Eng.* **2016**, *4*, 6391; d) H. Xie, C. P. Yang, K. Fu, Y. G. Yao, F. Jiang, E. Hitz, B. Y. Liu, S. Wang, L. B. Hu, *Adv. Energy Mater.* **2018**, *8*, 1703474.
[71] S. J. Chun, E. S. Choi, E. H. Lee, J. H. Kim, S. Y. Lee, S. Y. Lee, *J. Mater. Chem.* **2012**, *22*, 16618.
[72] J. H. Kim, J. H. Kim, E. S. Choi, H. K. Yu, J. H. Kim, Q. L. Wu, S. J. Chun, S. Y. Lee, S. Y. Lee, *J. Power Sources* **2013**, *242*, 533.
[73] a) K. Uetani, K. Hatori, *Sci. Technol. Adv. Mater.* **2017**, *18*, 877; b) N. Yildirim, S. M. Shaler, D. J. Gardner, R. Rice, D. W. Bousfield, *Cellulose* **2014**, *21*, 4337.
[74] F. Martoïa, T. Cochereau, P. J. J. Dumont, L. Orgéas, M. Terrien, M. N. Belgacem, *Mater. Des.* **2016**, *104*, 376.
[75] Y. Kobayashi, T. Saito, A. Isogai, *Angew. Chem., Int. Ed.* **2014**, *53*, 10394.
[76] J. Fu, S. Wang, C. He, Z. Lu, J. Huang, Z. Chen, *Carbohydr. Polym.* **2016**, *147*, 89.
[77] W. Chen, Q. Li, Y. Wang, X. Yi, J. Zeng, H. Yu, Y. Liu, J. Li, *ChemSusChem* **2014**, *7*, 154.
[78] D. Bendahou, A. Bendahou, B. Seantier, Y. Grohens, H. Kaddami, *Ind. Crops Prod.* **2015**, *65*, 374.
[79] C. Jimenez-Saelices, B. Seantier, B. Cathala, Y. Grohens, *Carbohydr. Polym.* **2017**, *157*, 105.
[80] L. J. Gibson, M. F. Ashby, C. Solids, *Structure and Properties*, Cambridge University Press, Cambridge **1999**.
[81] S. Deville, *J. Mater. Res.* **2013**, *28*, 2202.
[82] K. Sakai, Y. Kobayashi, T. Saito, A. Isogai, *Sci. Rep.* **2016**, *6*, 20434.
[83] L. W. Hrubesh, R. W. Pekala, *J. Mater. Res.* **1994**, *9*, 731.
[84] P. Munier, K. Gordeyeva, L. Bergstrom, A. B. Fall, *Biomacromolecules* **2016**, *17*, 1875.
[85] S. Gupta, F. Martoia, L. Orgeas, P. J. J. Dumont, *Appl. Sci.* **2018**, *8*, 2463.
[86] K. J. De France, T. Hoare, E. D. Cranston, *Chem. Mater.* **2017**, *29*, 4609.
[87] T. Nissilä, S. S. Karhula, S. Saarakkala, K. Oksman, *Compos. Sci. Technol.* **2018**, *155*, 64.
[88] T. Zhai, Q. Zheng, Z. Cai, L. S. Turng, H. Xia, S. Gong, *ACS Appl. Mater. Interfaces* **2015**, *7*, 7436.
[89] A. Balea, E. Fuente, A. Blanco, C. Negro, *Polymers* **2019**, *11*, 518.
[90] V. da Costa Correia, S. F. Santos, R. Soares Teixeira, H. Savastano Jr., *Constr. Build. Mater.* **2018**, *160*, 376.
[91] L. Ferrara, S. R. Ferreira, M. d. Torre, V. Krelani, F. A. de Silva, R. D. T. Filho, in *Nanotechnology in Construction* (Eds: K. Sobolev, S. P. Shah), Springer International Publishing, Cham, Switzerland **2015**, p. 325.
[92] Y. Cao, P. Zavaterri, J. Youngblood, R. Moon, J. Weiss, *Cem. Concr. Compos.* **2015**, *56*, 73.
[93] L. Fu, J. Zhang, G. Yang, *Carbohydr. Polym.* **2013**, *92*, 1432.
[94] C. Jiang, G. S. Oporto, T. Zhong, J. Jaczynski, *Cellulose* **2016**, *23*, 713.
[95] J. Zhao, C. Lu, X. He, X. Zhang, W. Zhang, X. Zhang, *ACS Appl. Mater. Interfaces* **2015**, *7*, 2607.
[96] S. Torgbo, P. Sukyai, *Appl. Mater. Today* **2018**, *11*, 34.
[97] Y. Qi, Z. Cheng, Z. Ye, H. Zhu, C. Aparicio, *ACS Appl. Mater. Interfaces* **2019**, *11*, 27598.

© 2021 Wiley-VCH GmbH

[98] S. Bose, M. Roy, A. Bandyopadhyay, *Trends Biotechnol.* **2012**, *30*, 546.
[99] Z. Li, X. G. Lv, S. Y. Chen, B. X. Wang, C. Feng, Y. M. Xu, H. P. Wang, *RSC Adv.* **2016**, *6*, 42229.
[100] X. Zhang, C. Wang, M. Liao, L. Dai, Y. Tang, H. Zhang, P. Coates, F. Sefat, L. Zheng, J. Song, Z. Zheng, D. Zhao, M. Yang, W. Zhang, P. Ji, *Carbohydr. Polym.* **2019**, *213*, 27.
[101] a) X. He, Q. Xiao, C. Lu, Y. Wang, X. Zhang, J. Zhao, W. Zhang, X. Zhang, Y. Deng, *Biomacromolecules* **2014**, *15*, 618; b) G. Li, A. G. Nandgaonkar, Y. Habibi, W. E. Krause, Q. Wei, L. A. Lucia, *RSC Adv.* **2017**, *7*, 13678; c) N. Naseri, J. M. Poirier, L. Girandon, M. Frohlich, K. Oksman, A. P. Mathew, *RSC Adv.* **2016**, *6*, 5999.
[102] H. S. Barud, R. M. N. Assuncao, M. A. U. Martines, J. Dexpert-Ghys, R. F. C. Marques, Y. Messaddeq, S. J. L. Ribeiro, *J. Sol-Gel Sci. Technol.* **2008**, *46*, 363.
[103] X. Li, S. Y. Chen, W. L. Hu, S. K. Shi, W. Shen, X. Zhang, H. P. Wang, *Carbohydr. Polym.* **2009**, *76*, 509.
[104] S. Ifuku, M. Tsuji, M. Morimoto, H. Saimoto, H. Yano, *Biomacromolecules* **2009**, *10*, 2714.
[105] R. Xiong, H. S. Kim, S. Zhang, S. Kim, V. F. Korolovych, R. Ma, Y. G. Yingling, C. Lu, V. V. Tsukruk, *ACS Nano* **2017**, *11*, 12008.
[106] M. Giese, L. K. Blusch, M. K. Khan, W. Y. Hamad, M. J. Maclachlan, *Angew. Chem., Int. Ed.* **2014**, *53*, 8880.
[107] a) Y. Habibi, L. A. Lucia, O. J. Rojas, *Chem. Rev.* **2010**, *110*, 3479; b) E. Lizundia, D. Puglia, T. D. Nguyen, I. Armentano, *Prog. Mater. Sci.* **2020**, *112*, 100668.
[108] a) M. Wysokowski, M. Motylenko, H. Stocker, V. V. Bazhenov, E. Langer, A. Dobrowolska, K. Czaczyk, R. Galli, A. L. Stelling, T. Behm, L. Klapiszewski, D. Ambrozewicz, M. Nowacka, S. L. Molodtsov, B. Abendroth, D. C. Meyer, K. J. Kurzydlowski, T. Jesionowski, H. Ehrlich, *J. Mater. Chem. B* **2013**, *1*, 6469; b) M. Wysokowski, I. Petrenko, A. L. Stelling, D. Stawski, T. Jesionowski, H. Ehrlich, *Polymers* **2015**, *7*, 235.
[109] J. L. Shamshina, P. Berton, R. D. Rogers, *ACS Sustainable Chem. Eng.* **2019**, *7*, 6444.
[110] a) G. Chu, W. Xu, D. Qu, Y. Wang, H. W. Song, Y. Xu, *J. Mater. Chem. C* **2014**, *2*, 9189; b) K. E. Shopsowitz, A. Stahl, W. Y. Hamad, M. J. MacLachlan, *Angew. Chem., Int. Ed.* **2012**, *51*, 6886.
[111] H. Xiao, W. Zhang, Y. Wei, L. Chen, *Cellulose* **2018**, *25*, 1809.
[112] a) K. Li, P. Berton, S. P. Kelley, R. D. Rogers, *Biomacromolecules* **2018**, *19*, 3291; b) Y. Wang, L. Zhang, A. Lu, *ACS Appl. Mater. Interfaces* **2019**, *11*, 41710; c) H. Jiang, K. Tovar-Carrillo, T. Kobayashi, *Ultrason. Sonochem.* **2016**, *32*, 398.
[113] a) C. Jia, C. Chen, Y. Kuang, K. Fu, Y. Wang, Y. Yao, S. Kronthal, E. Hitz, J. Song, F. Xu, B. Liu, L. Hu, *Adv. Mater.* **2018**, *30*, 1801347; b) J. Song, C. Chen, C. Wang, Y. Kuang, Y. Li, F. Jiang, Y. Li, E. Hitz, Y. Zhang, B. Liu, A. Gong, H. Bian, J. Y. Zhu, J. Zhang, J. Li, L. Hu, *ACS Appl. Mater. Interfaces* **2017**, *9*, 23520; c) J. Song, C. Chen, S. Zhu, M. Zhu, J. Dai, U. Ray, Y. Li, Y. Kuang, Y. Li, N. Quispe, Y. Yao, A. Gong, U. H. Leiste, H. A. Bruck, J. Y. Zhu, A. Vellore, H. Li, M. L. Minus, Z. Jia, A. Martini, T. Li, L. Hu, *Nature* **2018**, *554*, 224.

Meghan E. Lamm is a postdoctoral research associate in the Manufacturing Science Division of Oak Ridge National Laboratory (ORNL). She received her B.A. (2015) from Illinois Wesleyan University and Ph.D. (2019) in organic chemistry from the University of South Carolina, where her research focused on macromolecular engineering of biomass polymers. Her current research interests include development of novel polymeric materials for a range of applications including composite materials, biopolymers, polymer upcycling, and stimuli-responsive materials.

Nathalie Lavoine is an assistant professor of Renewable Materials Science in the Department of Forest Biomaterials at North Carolina State University (NCSU). Her research activities investigate the structure–processing–properties relationships of renewable nanotechnology for sustainable design and processing of advanced sustainable materials from the biomass, as crucial alternatives to fossil-fuel-based plastics. She received her Ph.D. in 2013 at the Laboratory of Pulp and Paper Sciences and Graphic Arts (LGP2), in France. She did two postdoctoral experiences, one at the University of Tokyo (Japan), as part of the research group of Prof. Isogai (2014–2016); the other at Stockholm University (Sweden) in the research group of Prof. Bergstrom (2016–2018).

© 2021 Wiley-VCH GmbH

Douglas J. Gardner is a professor and program leader of Forest Operations, Bioproducts and Bioenergy in the School of Forest Resources at the University of Maine. He is also a member of the Advanced Structures and Composites Center and Forest Bioproducts Research Institute. His research, teaching, and service activities focus on polymer and interfacial science aspects of wood–polymer composite materials.

Teng Li is currently the Keystone professor in the Department of Mechanical Engineering at the University of Maryland, College Park, where he directs the Laboratory for Advanced Sustainable Materials and Technology. He received his B.S. from Tsinghua University, M.A. from Princeton University, and Ph.D. from Harvard University. His current research interests include sustainable materials, low-dimensional nanomaterials, energy storage materials, soft materials, and flexible/stretchable electronics.

Liangbing Hu received his B.S. degree in applied physics from the University of Science and Technology of China (USTC) in 2002. He did his Ph.D. at the University of California, Los Angeles. In 2006, he joined Unidym, Inc. as a cofounding scientist. He did his postdoctoral studies at Stanford University from 2009 to 2011. Currently, he is a Herbert Rabin distinguished professor at the University of Maryland, College Park, and the director of the Center for Materials Innovation (CMI). His research interests include emerging energy storage technologies, sustainable nanomaterials for energy and environmental applications, and ultrahigh temperature manufacturing.

Soydan Ozcan is a senior R&D scientist and trust leader of Sustainable Composite Materials and Manufacturing at the Manufacturing Demonstration Facility of the Oak Ridge National Laboratory. His research addresses novel, high-value biomaterials from renewables and viable processes for their composite and additive manufacturing applications. He also facilitates the development of composite recycling technologies.

© 2021 Wiley-VCH GmbH